



## Nanodiamond-Based Sensing: A revolution for biosensors in capturing elusive bio-signals in living cells<sup>☆</sup>

Jiahua Zhang<sup>a,1</sup>, Linjie Ma<sup>a,1</sup>, Yong Hou<sup>a</sup>, Haoyi Ouyang<sup>a</sup>, Hyunsik Hong<sup>b</sup>, Kanghyeon Kim<sup>b</sup>, Heemin Kang<sup>b,c,\*</sup>, Zhiqin Chu<sup>a,d,e,\*</sup>

<sup>a</sup> Department of Electrical and Electronic Engineering, The University of Hong Kong, Hong Kong, China

<sup>b</sup> Department of Materials Science and Engineering and College of Medicine, Korea University, Seoul 02841, Republic of Korea

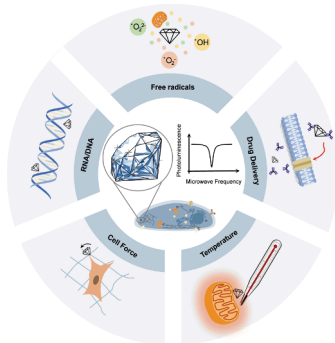
<sup>c</sup> College of Medicine, Korea University, Seoul 02841, Republic of Korea

<sup>d</sup> School of Biomedical Sciences, The University of Hong Kong, Hong Kong, China

<sup>e</sup> Advanced Biomedical Instrumentation Centre, Hong Kong Science Park, Shatin, Hong Kong, China



### GRAPHICAL ABSTRACT



### ARTICLE INFO

#### Keywords:

Nanodiamond  
Quantum sensor  
Elusive bio-signal  
Nanocarrier  
Drug delivery

### ABSTRACT

Cells constantly produce elusive bio-signals, such as cellular forces, free radicals, and molecular interactions, that are important for understanding diseases and treatment effects. However, detecting these signals is challenging because of issues with sensitivity, specificity, and the complexity of biological systems. Owing to their unique properties, nanodiamonds have emerged as a promising platform for detecting such elusive bio-signals, providing enhanced precision and effectiveness in diagnostics and therapies. In this review, we explore the detection of intracellular elusive bio-signals using nitrogen-vacancy (NV) centers in nanodiamonds, presenting case studies on their applications in cell force, free radicals, molecular interactions, and nanoscale thermometry. Moreover, we explore the design and applications of nanodiamonds as nanocarriers in quantum sensors and drug delivery systems.

<sup>☆</sup> This article is part of a special issue entitled: 'Carbon-Based Nano' published in Advanced Drug Delivery Reviews.

<sup>\*</sup> Corresponding authors.

E-mail addresses: [heeminkang@korea.ac.kr](mailto:heeminkang@korea.ac.kr) (H. Kang), [zqchu@eee.hku.hk](mailto:zqchu@eee.hku.hk) (Z. Chu).

<sup>1</sup> These authors made equal contributions to this work.

## 1. Introduction

Cells serve as intricate biochemical reactors, continuously producing a diverse array of bio-signals, including changes in ion concentration [1–5], cellular signalling molecules [6–8], membrane potential fluctuations [9,10], and temperature variations [11,12]. These signals underpin crucial cellular processes, ranging from molecular activities [13–16] such as DNA transcription, translation, and ATP hydrolysis to cellular dynamics [17–21] like division, adhesion, and migration. At a broader scale, they influence organism-level phenomena, including embryonic development [22,23] and muscle contractions [24,25]. Detecting these bio-signals with high-sensitivity and precision is vital for deepening our understanding of fundamental cellular processes and diseases progression. However, the elusive nature of many bio-signals, characterized by low intensities and their occurrence within complex, noisy cellular environments, presents significant challenges for existing detection technologies [26,27].

Over recent decades, advancements in live cell sensing have introduced techniques based on optical [28], electronic [29], fluorescent [30], and magnetic [31,32] technologies. These approaches have enhanced our ability to observe cellular dynamics [33]. Yet, they face limitations in sensitivity, stability, and specificity. Issues like photo-bleaching, cytotoxicity, and interference from environmental factors, such as pH changes or autofluorescence, compromise their effectiveness. These shortcomings highlight the urgent need for innovative technologies capable of delivering stable, high-precision measurements in the complex physiological settings of living cells.

Nanodiamonds, particularly those embedded with nitrogen-vacancy

(NV) centers, offer a promising solution for detecting elusive bio-signals in living cells. Their unique quantum properties, derived from NV centers, allow for the precise detection of subtle bio-signals, such as nanoscale cellular forces, free radicals [34], that conventional methods [35] often overlook. This quantum-based approach delivers exceptional precision and spatiotemporal resolution, surpassing the limitation of traditional sensors, which struggle to maintain accuracy in the complex and dynamic conditions of living cells. For example, nanodiamonds can capture transient phenomena, like spin fluctuations [34] in free radicals, without the irreversibility and degradation that hinder fluorescent labelling techniques. Moreover, by leveraging their quantum properties, nanodiamonds enable background-free imaging [36], critical for isolating specific bio-signals from surrounding biological noise. Beyond sensing, nanodiamonds exhibit exceptional photostability, biocompatibility, and ease of functionalization, making them highly adaptable for biomedical applications. These qualities position them as an ideal platform not only for imaging and sensing but also for drug delivery and integration into practical systems like microfluidic devices and lateral flow assays [37], enhancing their utility in rapid diagnostics.

This review focuses on cutting-edge detection technologies utilizing NV centers in diamonds to measure elusive intracellular bio-signals, such as nanoscale cellular forces, radicals, biomacromolecules, and temperature (Fig. 1). We begin by briefly outlining the general limitations of mainstream detection methods, namely their struggles with sensitivity, stability, and specificity in complex environments. Next, we provide an in-depth exploration of the technical features of NV-based quantum sensing, emphasizing its unique advantages for detecting these signals, illustrated by specific case studies and forward-looking

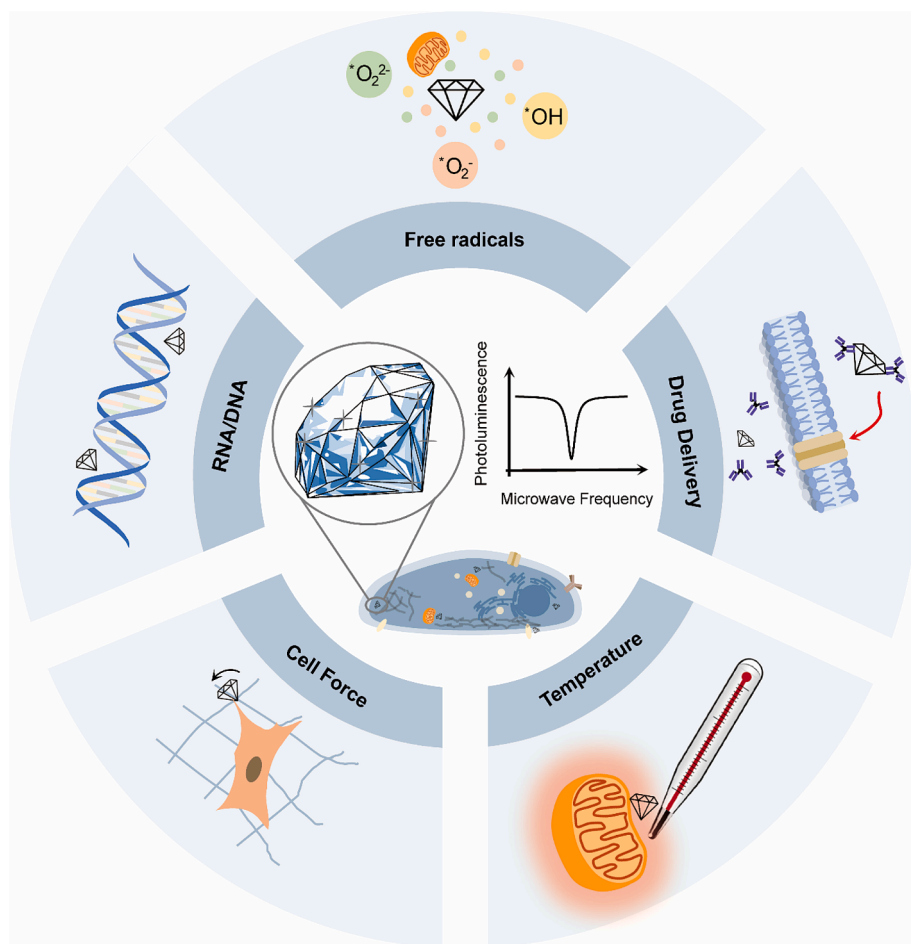


**Fig. 1.** Nanodiamond sensors can detect elusive biosignals in living cells such as temperature, free radicals, cell force, and small molecules such as RNA and DNA. Further they can serve as drug-delivery system.

insights into the field's future developments (Table 1). Lastly, we explore the design and applications of nanodiamonds as nanocarriers in next-generation diamond-based quantum sensors and drug delivery systems.

## 2. Diamond-Based sensing technology using NV centers

Color centers in diamonds represent point defects where an impurity atom substitutes a carbon atom within the lattice, enabling to absorb specific wavelengths of light and generate fluorescence. Among these, the negatively charged NV<sup>-</sup> center (unless specified, NV refers to the negative charge state NV<sup>-</sup> in this review) in diamond [38] has been extensively explored for quantum sensing and bio-imaging applications [31,39,40].

### 2.1. Diamond-based sensor

Diamond, the host of the NV center, is famous for its outstanding properties. These include high mechanical stability, biocompatibility, chemical inertness, thermal conductivity, and transparency. Such traits make it an ideal platform for quantum sensing in biological systems. Single-crystalline diamond outperforms polycrystalline diamond in sensitivity for quantum sensing. Based on the physical size, diamond used in biosensing are classified as nanodiamond [41] or bulk diamond (films/plates/wafers) [42]. Nanodiamonds ranges from several nanometers (for hosting NV center stably) to hundreds of nanometers. Combined with excellent biocompatibility and great potential of surface functionality (Fig. 2b), it has been used in biosensing and drug delivery and shows a promising future. Bulk diamond, synthesized by High-Pressure High-Temperature (HPHT) or Chemical Vapor Deposition (CVD), suit widefield sensing due to their relatively large scale.

Although natural diamonds contain NV centers, their density is often too low for practical applications. Moreover, the NV centers in natural diamonds are randomly distributed. While this is acceptable in many cases, shallow NV centers are preferred as they can provide better sensing sensitivity. Artificial implantation of NV centers is an effective solution. The creation of NV centers involves introducing nitrogen atoms—either through doping or ion implantation—and generating vacancies within the diamond lattice. An annealing process, which enables the diffusion of the vacancy, is also required for the formation of the NV center at the end of the process. These processes allow precise control over both the density and depth of NV centers.

However, shallow NV centers are unstable due to the charge instability and magnetic and electronic noise. Charge instability is due to the

light-induced charge state transit between NV<sup>0</sup> and NV<sup>-</sup> state. As the NV<sup>0</sup> state cannot be used for quantum sensing, the generation of NV<sup>0</sup> state will cause extra fluorescence background, leading to a decrease of the signal contrast. Magnetic and electronic noise comes from the proximal spins and unscreened charge, these will influence the quantum property, such as  $T_2$  (transversal relaxation time), of the NV center. Suitable surface functionalization can be used to increase the stability of the NV center. Oxygen-terminate, such as hydroxyl (C-OH), carboxylic acid (COOH), carbonyl (C=O), and ether (C-O-C) groups, are good choose as they not only increase the stability of the NV centers [44] but also provide the potential for subsequent chemical functionalization.

### 2.2. Optical Properties-based sensing

The NV center can be excited across a broad wavelength range from 450 to 637 nm. Green laser light (532 nm) is preferred for its high excitation efficiency. When excited, the NV center emits a broadband fluorescence spectrum ranging from 600 to 800 nm, as shown in Fig. 2d. This range, spanning visible and near-infrared, making it an ideal biomarker for imaging. Notably, the NV center has outstanding exceptional photostability, distinguishing it from traditional fluorescence dyes, semiconductor quantum dots, carbon dots, fluorescent beads, and other fluorescent nanoparticles [45].

The zero-phonon line (ZPL) at around 637 nm is a distinctive feature of the NV fluorescence spectrum. It reflects electronic transition devoid of phonon interaction. ZPL width and intensity provide insights into the local environment of the color centers. With an increase in temperatures, phonon interactions broaden ZPL width and diminish its intensity, enabling the monitoring of temperature fluctuations at the nanoscale [46].

The excitation efficiency of the NV center depends on the coupling between its electric dipoles and the polarization of the excitation laser. Previous studies have revealed that the NV center possesses two orthogonal electric dipoles lying in a plane perpendicular to the NV axis [47]. As the two electric dipoles are perpendicular to the NV axis, the optical polarization anisotropy varies with direction. When the NV axis aligns with the laser transmission direction, the polarization of the laser will show no effect on the overall intensity. In contrast, when the NV axis forms an angle ( $\phi$ ) with the laser transmission direction, the effective excitation efficient is contingent on the relative angle ( $\theta$ ) between the laser polarization and the projection of the NV axis onto the laser polarization surface, which result in the polarization modulation of the fluorescence intensity [48]. By analysing fluorescence polarization curves, as shown in Figure X, researchers can determine the orientation

**Table 1**  
Comparison the performance between traditional sensing technologies and nanodiamond-based sensing methods.

	Traditional	Nanodiamond-based		Potential Application field
		Method	Advantages	
Cellular adhesion forces	Förster resonance energy transfer (FRET)	T1	Low photobleaching; Easy data interpretation	Mechanobiology; Tissue development; Mechano-drug development
Cellular torsional forces	NA	Polarization	Quantitative measurement of rotation angle	Cell-matrix interactions; Mechanobiology;
Free radical	Measure the damage that radicals cause to the lipids, proteins, and nucleic acids of the cells; Uses fluorescent or spin labels that react with radicals to form a fluorescent molecule	T1	Highly sensitive; High spatial resolution; Enable long-term dynamic measurement; High chemical stability; High photo stability	Disease diagnosis(Alzheimers Disease (AD), Parkinson's Disease (PD), Cancer); Cell aging study; Drug screening
RNA/DNA	Polymerase chain reaction (PCR)	T1 Fluorescence	Highly sensitive; Rapid test; Portable test; Simple setup	Cancers and viral infections; Elucidate the structure of single biomolecules and their intermolecular interactions
Temperature	Thermosensitive fluorescent dyes; Quantum dots; Upconversion Nanoparticles	CW-ODMR	Highly accuracy; Stable; High spatial resolution	Thermotherapy; Cellular metabolism evaluation; Disease diagnosis (Inflammation, Cancer)

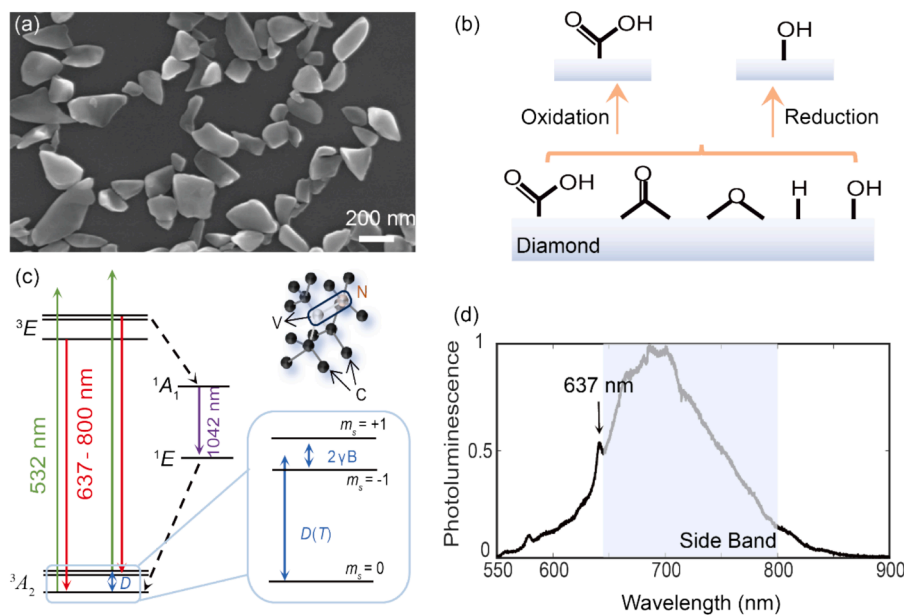


**Fig. 2.** Properties of NV centers. (a) TEM image of nanodiamonds. [43] (b) Surface chemical functionalization. (c) Energy level and atomic structure. (d) Fluorescence spectrum.

of the NV axis [49].

### 2.3. Spin Properties-based sensing

The energy level structure of the NV center [50] is shown in Fig. 2b. Within the diamond lattice, the NV center comprises a spin-1 system characterized by a spin triplet ground state. As the  $m_s = 0$  sublevel exhibits greater brightness than the  $m_s = \pm 1$  spin sublevel, it enables optical differentiation between the two spin states based on their distinct fluorescence intensities. In the absence of an external magnetic field, the energy levels of the NV-center electrons in the  $m_s = \pm 1$  state merge. However, upon the introduction of an external magnetic field, the NV spin experiences Zeeman splitting, causing the  $m_s = \pm 1$  energy level to degenerate.

Optically detected magnetic resonance (ODMR) is a versatile technique that leverages the fluorescence of NV centers to monitor changes in their spin states. This method is applicable across a wide temperature

range, spanning from ultra-low temperatures of 350 mK [51] to high temperatures of up to 1000 K [52]. Notably, pioneering studies have used ODMR to identify and analyze chains of magnetic nanoparticles (magnetosomes) present in magnetotactic bacteria, showcasing the first step towards potential biological applications of this technology [31]. To perform the ODMR experiment, the NV center is excited from the ground state to the excited state by a 532 nm laser. Afterward, it decays back to the ground state. During this process,  $m_s = 0$  state conserve, but  $m_s = \pm 1$  states have a higher possibility of decaying into  $m_s = 0$  state, causes the most of NV centers end up in  $m_s = 0$  state after several excitation loops. By applying an external microwave field, the occupation of sublevels within the NV centers can be manipulated. When the microwave frequency matches the resonant frequency for transitions such as  $m_s = 0$  to  $m_s = -1$  or  $m_s = 0$  to  $m_s = +1$ , the NV fluorescent signal significantly decreases because of the disparate brightness of the  $m_s = 0$  and  $m_s = \pm 1$  sublevel, allowing the acquisition of the NV resonance spectrum. ODMR experiments can be carried out under both continuous-

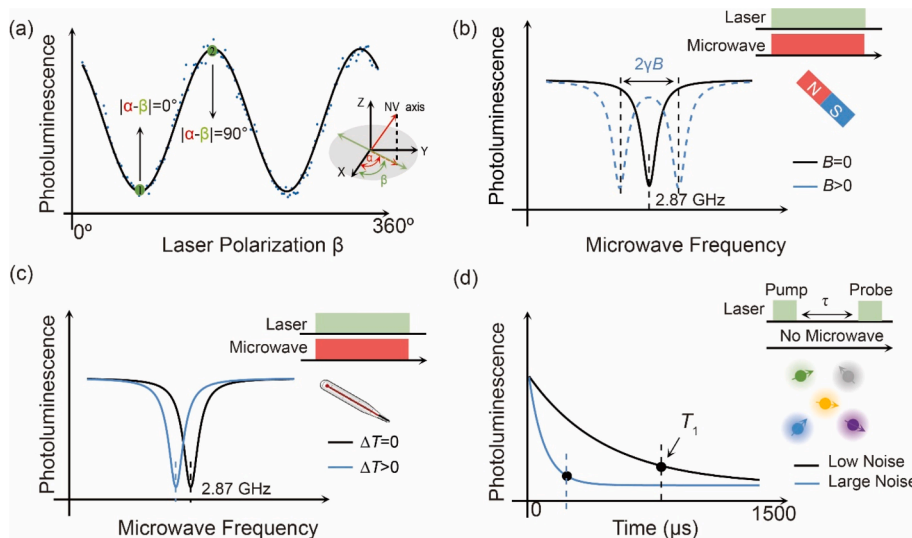


**Fig. 3.** NV centers based popular measurement technologies. (a) Fluorescence polarization curves and relation between NV axis orientation and laser polarization. (b) ODMR without and with magnetic field. (c) ODMR at different temperature. (d)  $T_1$ .

wave (CW-ODMR) and pulsed mode (pulsed-ODMR). The former are technically simpler and offer higher photon counts; the latter has more technical complexity but can offer a higher contrast ratio, leading to better signal-to-noise ratio (SNR).

Both CW-ODMR and pulse-ODMR can be applied for measuring magnetic fields and temperatures [53] (Fig. 3b and Fig. 3c). In this review, only CW-ODMR is introduced, as it achieves a balance between methodological complexity and measurement accuracy. Readers can refer to [54] for more details of pulsed ODMR.

Fig. 3b shows the laser and microwave sequence for CW-ODMR and the corresponding signal. To measure the CW-ODMR spectrum, the excitation laser and microwave field remain continuously on while the microwave frequency is swept over a specified range. The fluorescence intensity of the NV center is recorded as a function of the microwave frequency, yielding the CW-ODMR spectrum.

The Longitudinal relaxation time ( $T_1$ ) of NV centers, indicative of the spin system's rate of return to thermal equilibrium, can be assessed with or without microwave excitation. This method involves initially polarizing the NV spin to the polarized state ( $m_s = 0$  and  $m_s = \pm 1$ ), allowing the NV electrons to freely evolve towards the thermal equilibrium state ( $m_s = 0$  and  $m_s = \pm 1$  with equal probability), and determining  $T_1$ .  $T_1$  is influenced by magnetic noise within the NV environment arising from both internal defective atoms in the NV centers and external sources. Elevated noise levels lead to more significant perturbations, resulting in a faster relaxation rate and shorter  $T_1$ .

Fig. 3d shows the laser and microwave sequence for  $T_1$  and the corresponding signal. Notably,  $T_1$  can be measured without microwave excitation, which requires simple pulse sequence. The spin state of the NV center is first initialized to  $m_s = 0$  using a laser pulse of approximately 2 microseconds. After a free relaxation period of duration  $\tau$ , another laser pulse is applied to read out the current spin state. The fluorescence intensity varies with the free relaxation time  $\tau$ , and  $T_1$  is determined by fitting the time-dependent fluorescence intensity curve using formula  $I_t = I_{max}(1 - e^{-\tau/T_1})$ , where  $I$  represent the fluorescence intensity. If low-frequency noise cancellation is needed, the reader can refer to [54] for sequence of  $T_1$  measurement with microwave. Microwave-free  $T_1$  measurements have been applied in the biological domain for detecting magnetic signals, pH levels, and temperature variations [55]. Understanding  $T_1$  is crucial for delineating spin dynamics and enhancing the performance of NV-based sensors.

The transverse relaxation time ( $T_2$ ) is indicative of the coherence duration of NV center spins and plays a pivotal role in quantum sensing applications. Specifically, the sensitivity of measurements involving alternating magnetic fields is determined by the coherence time, represented by  $T_2$ . In this method, the NV spin is polarized to the  $m_s = 0$  state, followed by the application of a  $\pi/2$  pulse to maintain the NV spin in the  $m_s = 0$  and  $m_s = 1$  superposition state, allowing the quantum state to evolve freely. Subsequently, a  $\pi$  pulse is employed to counteract the phase accumulation of electron spins during the evolutions, effectively mitigating constant-value and low-frequency magnetic noise and preserving the coherent spin state. A subsequent  $\pi/2$  pulse facilitates the conversion of phase information into readable data, allowing the determination of  $T_2$ . The nitrogen concentration within the NV environment affects  $T_2$ , which exhibits an inverse linear relationship with nitrogen concentration exceeding 0.5 ppm [56]. Moreover, NV centers hold promise for applications in nanoscale NMR spectroscopy and imaging, facilitating investigations into magnetic fields at the molecular level, such as intraprotein structure [57]. A more complicated spin-control sequence is needed for  $T_2$ , readers can refer to [54] for more details.

### 3. Nanodiamond-Based sensing of elusive Bio-Signals for diagnostic and therapeutic Applications

#### 3.1. Cell force

Cells live in dynamic environment, facing extrinsic mechanical cues such as shear, tensile, and compressive forces. In response, cell constantly generate forces and dictate their behaviours to maintain tissue-level structural integrity and functionality. Therefore, capturing and quantifying such cell forces with high precision is critical for gaining insights into cellular behaviours [58], tissue mechanics [59–61], disease development [62] and treatment effectiveness [63–65]. Over the past few decades, notable achievements have been made using deformable hydrogels, microfabricated substrates, and devices that visualize and quantify these forces through the wrinkling of silicone rubber substrates and traction force microscopy (TFM). Although the spatiotemporal resolution of these technologies has been greatly improved due to advancements in super-resolution technology and algorithms, detecting molecular force dynamics is still beyond current capabilities, hindering a deeper understanding of the molecular mechanisms of mechanotransduction.

Single-molecule tension microscope (SMTM) have gained significant attention for their ability to measure the forces experienced by specific proteins. Commercialized equipment such as atomic force microscopy, magnetic tweezers, and optical tweezers can provide solutions but require specialized equipment, and their low throughput limits their applicability. Molecular tension fluorescence microscopy is a cutting-edge method in this field; it uses a “spectroscopic ruler” based on energy transfer between a fluorophore and a quencher. The main mechanisms involved are Förster resonance energy transfer (FRET) and nanometal surface energy transfer. However, these powerful techniques suffer from low SNR, fluorophore photobleaching, and challenges in force calibration.

Diamond-based force-sensing technology provides a promising solution to these challenges. The exceptional optical stability of diamond greatly reduces photobleaching effects. By combining next-generation quantum measurement platforms with innovative bio-interface engineering technologies, researchers developed an effective method termed quantum-enhanced diamond molecular tension microscopy (DQMTM) to precisely measure cellular adhesion forces [66]. The core technology utilized in this tool is NV color center-based  $T_1$  relaxometry, which provides high-resolution magnetic noise sensing and imaging (Fig. 4a). Meanwhile, the DQMTM is completely label-free, requiring no fluorophores. In principle, the optical stability of diamond and the high magnetic noise sensitivity of the NV center help overcome various challenges, such as photobleaching, limited sensitivity, and ambiguities in data interpretation.

Current cellular force measurement methods, including TFM and MTM, rely on measuring the linear displacement of the fluorescent beads embedded in elastic substrates or the one-dimensional extension of ‘spring-like’ ligands driven by cells. They have significantly enhance our understanding of the role of cellular forces in terms of “push” and “pull”, Nevertheless, they remain limited in addressing more complex and diverse mechanical interactions that involve multiple degrees of freedom, such as torsional stress. The dipole-like features of NV centers exhibit intriguing characteristics when subjected to polarized light, a phenomenon known as optical polarization selective excitation. Researchers harnessed this unique polarization property of NV centers in nanodiamonds as fluorescent orientation markers and developed a linear polarization modulation method to monitor the in-plane rotational motions of these nanodiamonds with high precision (Fig. 4b), achieving an accuracy of 0.5–3° [67]. This method can be applied to quantification of cellular torsional forces.

Although the application of diamond sensors in the field of cellular force measurement is still in its early stages, the potential of these sensors cannot be overlooked. With their unique properties, including

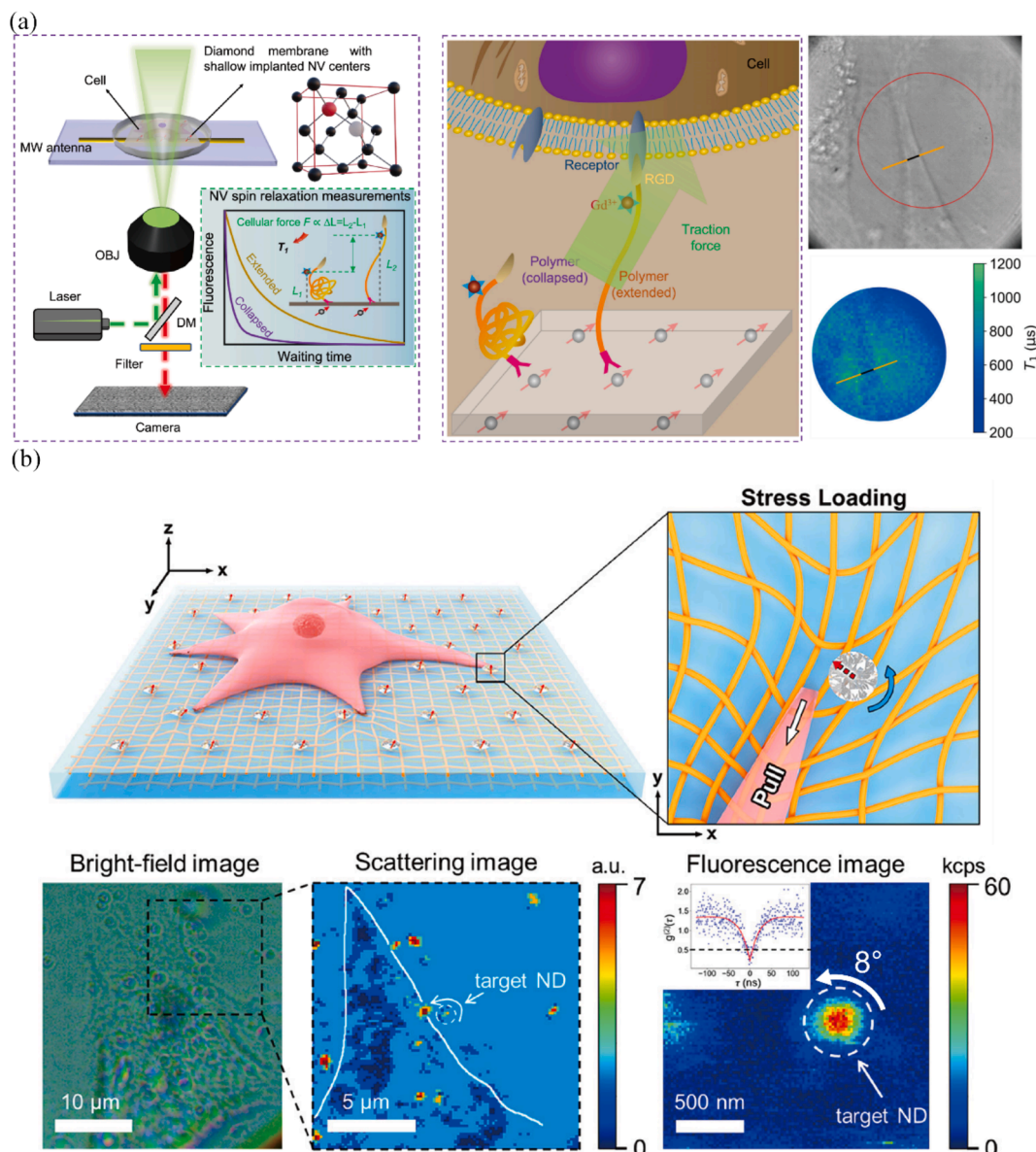


**Fig. 4.** Diamond-based cell force measurement. (a) Diamond-based sensor for monitoring cellular adhesion forces. The left panel illustrates polymer extension caused by cellular forces. The right panel demonstrates how changes in  $T_1$  values correlate with polymer extension, enabling measurement of cellular adhesion forces. The lower panels demonstrate the measured data [66]. (b) Diamond-based sensor for detecting PDMS rotation induced by cell traction forces. It illustrates how cell-driven substrate deformation results in the nanodiamond rotation [67].

exceptional long-term stability and reusability, diamond sensors have distinct advantages over conventional methods. Current diamond-based sensing has significant room for improvement in spatiotemporal resolution, diversity, and accessibility, we believe it represents a new technical roadmap for force sensing in mechanobiology, driven by rapid advancements in quantum sensing technology. Continued improvements will expand its capabilities, eventually establishing it as a fundamental tool in biomedical science. In future, diamond-based platforms can significantly enhance and complement existing technologies, driving advancements in the field of cellular biomechanics.

### 3.2. Free radicals

Free radicals are highly reactive molecules generated from nonenzymatic and enzymatic reactions in tissues. Endogenous free radicals originate in organelles like the endoplasmic reticulum, mitochondria, and peroxisomes. The most important free radicals generated during

metabolic reactions are oxygen-derived radicals, commonly known as reactive oxygen species (ROS). At moderate or low levels, ROS are beneficial to cells and contribute to various physiological functions. However, excess ROS can compromise the integrity of various biological molecules. Harman's free-radical theory of aging suggests that oxidative damage caused by ROS, which are generated throughout life, gradually accumulates, leading to cellular aging. Besides that, numerous diseases, such as cancer, cardiovascular disease, and neurodegenerative diseases, are associated with ROS [68]. Therefore, long-term quantitative ROS measurement at the molecular level within cells is of great importance, as it can provide evidence for early cellular damage and help to increase the understanding of cellular aging mechanisms.

Free radicals can be detected using direct and indirect methods. Indirect methods measure the damage that radicals cause to the lipids, proteins, and nucleic acids of the cells [69]; however, they cannot provide details of how the damage occurred or where the reactive molecules originated. Another approach involves measuring cellular

responses, but it lacks spatial and temporal resolution. The direct method uses fluorescent or spin labels that react with radicals to form a fluorescent molecule or a stable radical, which can be detected by fluorescence microscopy or magnetic resonance techniques. However, these labels are often used in relatively high concentrations, which can be cytotoxic. They can also suffer from instability caused by photo-bleaching and auto-oxidation. Moreover, they do not reflect the real-time condition of the sample, as the results stem from the cumulative effect of ROS.

The diamond-based free-radical sensor monitors ROS by measuring T1 of NV centers in diamonds (Fig. 5), which is sensitive to spin fluctuations induced by these species [34]. This method provides unique advantages for measuring intracellular ROS. First, it is both biocompatible and highly sensitive. Second, the use of micron- and nanoscale diamond particles significantly enhances the spatial resolution of ROS measurements [70]. Third, and more importantly, unlike traditional probes that react irreversibly with free radicals, diamond particles exhibit high chemical stability and are not consumed in the process. Finally, the photostability of NV centers in diamonds drastically reduces photobleaching, enabling long-term dynamic measurements.

In a preliminary study, nanodiamonds were used to measure phagocytic radical production by NADPH oxidase in primary dendritic cells [71]. This study demonstrated the potential for measuring intracellular free radicals. With the aid of diamond-based sensors, effects of external environmental factors, such as cell hypoxia and reoxygenation [72], ultraviolet B radiation [73], and cigarette smoke extract [74], on intracellular free radicals have been revealed.

Diamond-based sensors have emerged as powerful tools for studying free radicals-related disease diagnosis [75]. Cancer studies using diamond-based sensors have revealed that ROS influence the migratory potential of cancer cells, widening the opportunities for novel therapies [76]. Owing to the high spatial resolution provided by diamond-based sensors, free radicals have been found to be generated near polyglutamine aggregates in autolysosomes, which may be a cause or a consequence of the Huntington's disease phenotype [77]. Diamond-based sensors can also help determine the exact location and concentration fluctuations of free radicals in cells affected by viral infections, contributing to the development of strategies to combat viral infections [78]. A high spatial resolution is also important for revealing free

radical-related antibacterial mechanisms. Monitoring ROS levels near individual bacteria can enhance our understanding of how antibiotics kill bacteria [78] and the mechanisms by which some bacteria withstand oxidative stress [79].

In addition, diamond-based sensors can be used for drug screening by detecting the generation of ROS, offering insights into the therapeutic effects of drugs. Osteoarthritis and rheumatoid arthritis are two common types of arthritis. Piroxicam, a common nonsteroidal anti-inflammatory drug, has been shown to decrease free-radical levels in fibroblast-like synoviocytes from patients with osteoarthritis [80]. This finding helps to explain the drug's varying effectiveness in different diseases. Furthermore, diamond particles are ideal drug carriers, providing a powerful tool to not only deliver drugs but also measure their local effects [81].

Diamond sensors have shown promise in free-radical measurement. Besides their inherent stability and biocompatibility, they provide a spatiotemporal resolution far beyond that of conventional methods. With advancements in diamond sensor fabrication and measurement techniques, molecular-level free-radical measurement in biological systems is expected to become a useful strategy for studying biosignals in living cells. In the future, movement tracking of FNDs and pulsing experimental techniques could be utilized to identify specific free radical species. Additionally, reducing the variation in quantum sensing properties among sensors would further enhance sensing accuracy.

### 3.3. RNA and DNA

RNA and DNA are essential in diseases diagnosis and treatment. By detecting these molecules in a patient's body fluids or tissues, healthcare professionals can identify various conditions, including cancers and viral infections [82]. The polymerase chain reaction (PCR) is a widely used laboratory technique that amplifies specific DNA sequences through a series of temperature-dependent cycles of denaturation, annealing, and extension [83,84]. This powerful tool enables researchers to generate millions of copies from a minimal sample. For example, the most widely used real-time polymerase chain reaction assay can detect SARS-CoV-2 RNA from the upper respiratory tract to diagnose an active COVID-19 infection [85].

However, one significant drawback of PCR is its susceptibility to

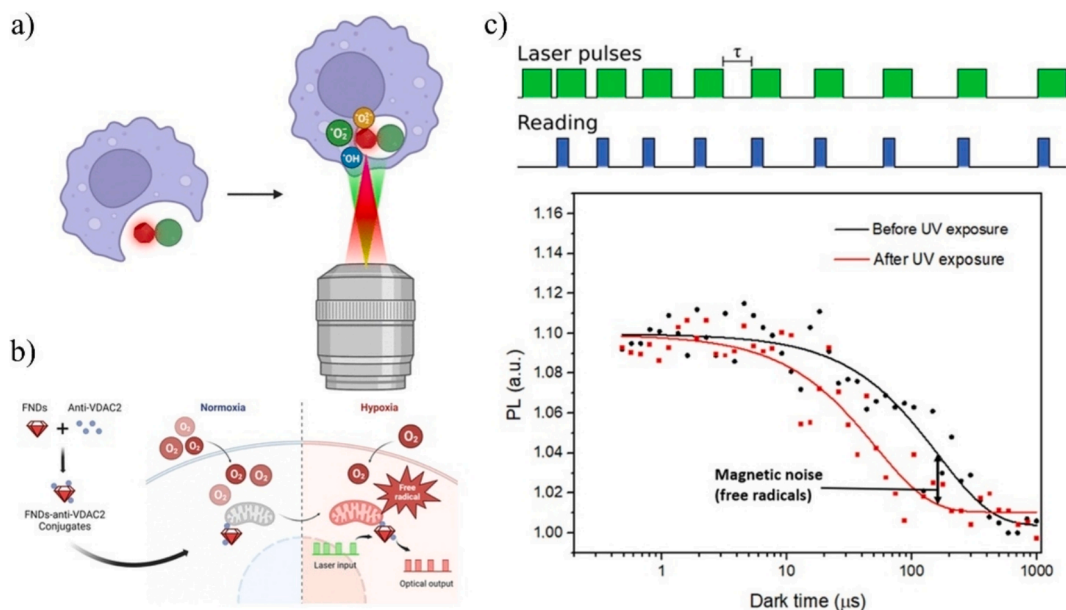


**Fig. 5.** Nanodiamond-based sensors for measuring free radicals. (a) schematic representation of intracellular free-radical measurement. the diamond particle, bound to a specific molecule, is internalized by cells to target the region of interest, allowing localized free-radical monitoring [79]. (b) Monitoring of free radicals produced by mitochondria using FNDs [72]. (c) T1 measurement pulse sequence (upper) [34] and relaxation response of diamond to free radicals (lower) [73].

false-negative results. Poor extraction methods may result in low yields and poor quality of target DNA, significantly affecting the outcome of PCR and contributing to false negatives [86]. The complexity of PCR protocols is also a disadvantage, as the need for precise temperature cycling and specialized equipment can limit its accessibility in resource-limited settings [87]. Additionally, PCR can be time-consuming and labour-intensive, especially when amplifying multiple targets simultaneously [88]. While PCR is an invaluable tool in molecular diagnostics and research, its disadvantages, including susceptibility to false negatives and operational complexity, hinder its suitability for current market needs. Currently, there is an increased demand in the market for high-precision and rapid point-of-care nucleic acid testing technologies, a trend that has been further intensified by the COVID-19 pandemic.

The most critical issue of rapid nucleic acid detection technology is sensitivity. For example, the sensitivity of paper microfluidic lateral flow assays (LFAs) [89,90], which are commonly utilized rapid point-of-care tests, is often hindered by background fluorescence stemming from the sample and substrate. However, when FNDs are employed as fluorescent markers in LFAs, their signal can be effectively distinguished from the background through selective spin modulation, thereby enabling highly sensitive testing (Fig. 6a). Furthermore, FND signals can be read optically with short acquisition times. These benefits render FND-based biosensors well-suited for quick, straightforward, and portable testing in clinical environments. In a notable study, researchers have integrated FNDs into a sandwich assay for oligonucleotide detection, achieving a detection limit of  $82 \times 10^{-21}$  M in a biotin-avidin model system (Fig. 6b) [37]. This sensitivity level is  $10^5$  times higher than that obtained using gold nanoparticles as fluorescent markers. Notably, the detection of single copies of human immunodeficiency virus type 1 (HIV-1) RNA is accomplished using 600-nm FNDs combined with a 10-minute reverse transcription-recombinase polymerase amplification (RT-RPA) assay (Fig. 6c).

Moreover, to enhance the sensitivity of bio-signal detection, FNDs can be used not only as fluorescence labels but also as quantum sensors to detect magnetic signals with high sensitivity. By incorporating external magnetic markers, biological signals are transformed into magnetic signals, thereby improving the sensitivity and precision of detection. In a specific demonstration, Gd<sup>3+</sup> functionalized nanodiamonds have been utilized for the detection of SARS-CoV-2, the virus responsible for COVID-19 (Fig. 6d and e) [91]. This method allows for the identification and quantification of viral RNA by optically monitoring changes in the relaxation time. It provides a rapid and reliable testing platform with a low FNR of 1 %, significantly lower than that of reverse transcriptase quantitative polymerase chain reaction, even in the absence of the RNA amplification process. In another demonstration, as shown in the Fig. 6f and g, using magnetic nanotags, researchers have established a hydrogel-based multiplexed magneto-DNA assay, featuring a remarkable detection limit in the attomolar range, exceeding those of conventional optical and electrochemical detection techniques [92]. While the above researches do not demonstrate the application in LFA format, their microfluidic platform experiments show promise in facilitating clinical diagnostic tests aimed at genetic mutations, rare diseases, and infections.

Currently, FNDs offer highly sensitive, reliable, rapid, simple, and portable testing in clinical settings. Beyond rapid point-of-care testing, FNDs also show promise in providing structural determination of intracellular single DNA and RNA through NMR [93]. Although the determination of single biomolecules, such as single DNA [94] or single protein [95], through NMR is still in its early stages, this research opens up the possibility of elucidating the structure of single biomolecules and their intermolecular interactions.

### 3.4. Temperature

Temperature profoundly influences the internal activities of living organisms, regulating physiological functions. Numerous studies have

explored the correlation between temperature variations and diverse functions in individual organisms, aiming to elucidate their molecular mechanisms. These studies reveal that, beyond the thermogenic properties of specific cells and organelles, temperature variation drives biological events. At the cellular level, for instance, adaptive changes in gene expression, such as the heat shock response and stress granule formation [96,97], protect cells from heat damage. Additionally, several ion channels, including transient receptor potential channels, are activated in a temperature-dependent manner [98,99]. In *Drosophila*, temperature-regulated behavior is closely linked to the rates of mitochondrial oxidative metabolism in cells [100]. These findings suggest that temperature variations at the cellular level are integral to physiological functions in living organisms. This understanding could enhance diagnostic and treatment strategies by targeting temperature-sensitive pathways in disease management.

While the biological significance of intracellular temperature changes is recognized, understanding the physical principles behind these changes remains elusive. Nanoscale fluorescence thermometry has been developed to measure temperature at the single-cell level, leading to advances in understanding the molecular mechanisms of temperature-related physiological functions. However, the specifics of heat release at subcellular resolution remain unclear, particularly in quantitative terms. A paradox known as the “ $10^5$  gap issue” exists in intracellular nanothermometry: calculated temperature rises are often orders of magnitude smaller than those observed experimentally. For instance, Baffou et al. estimated a temperature increase of approximately  $10^{-5}$  K within a single cell, based on assumptions about the heat source size (10  $\mu$ m) and previously reported cellular heat production (100 pW) [101]. This estimate is significantly lower than the roughly 1 K increase reported in the literature [11], which is thought to result from thermogenesis.

Several reasons contribute to the issue above. On the one hand, mainstream temperature measurement methods, such as those using fluorescent dyes, thermosensitive polymers, and nanoparticles, are still underdeveloped. They face several challenges, including photobleaching, limited long-term monitoring, and difficult calibration. Additionally, fluorescence is influenced by factors like refractive index, viscosity, optical excitation power, pH, salt concentration, and proteins, leading to potential measurement errors. On the other hand, the complexity of the intracellular microenvironment and thermal processes presents additional challenges. Variations in the thermal conductivity of cellular components, such as proteins and phospholipids, introduce errors in calculations and calibrations. Heat flow and temperature changes within cells can also impact chemical and physical processes, such as altering reaction equilibria, inducing particle movement, and forming pH gradients, thereby complicating intracellular temperature research.

Compared to other fluorescence nanothermometers, FNDs offer high sensitivity and high spatial resolution for temperature measurement. They also possess attractive fluorescent properties, including a high quantum yield and no blinking or photobleaching. Furthermore, FNDs are biocompatible with low cytotoxicity [102], and exhibit high stability in complex physiological environments. Additionally, FNDs can be biofunctionalized with surface groups and expanded for various biological applications [103].

In an initial experiment, nanodiamonds with NV centers were used for the quantitative detection of intracellular temperature increases at one location with a spatial resolution of 100 nm (Fig. 7a), using an external heat source (gold nanoparticles) based on ODMR [104]. They developed a four-point method to achieve a standard deviation of temperature around 0.1–0.2 K with a temporal resolution of 4 s in their measurements. They first demonstrated the high sensitivity and high spatial resolution in the measurements. Later, another group measured the intracellular temperature of a neuronal network (Fig. 7b) using widefield ODMR, achieving widefield temperature mapping [39]. In another demonstration, the four-point method was improved by minimizing measurement artifacts caused by optical power-dependent

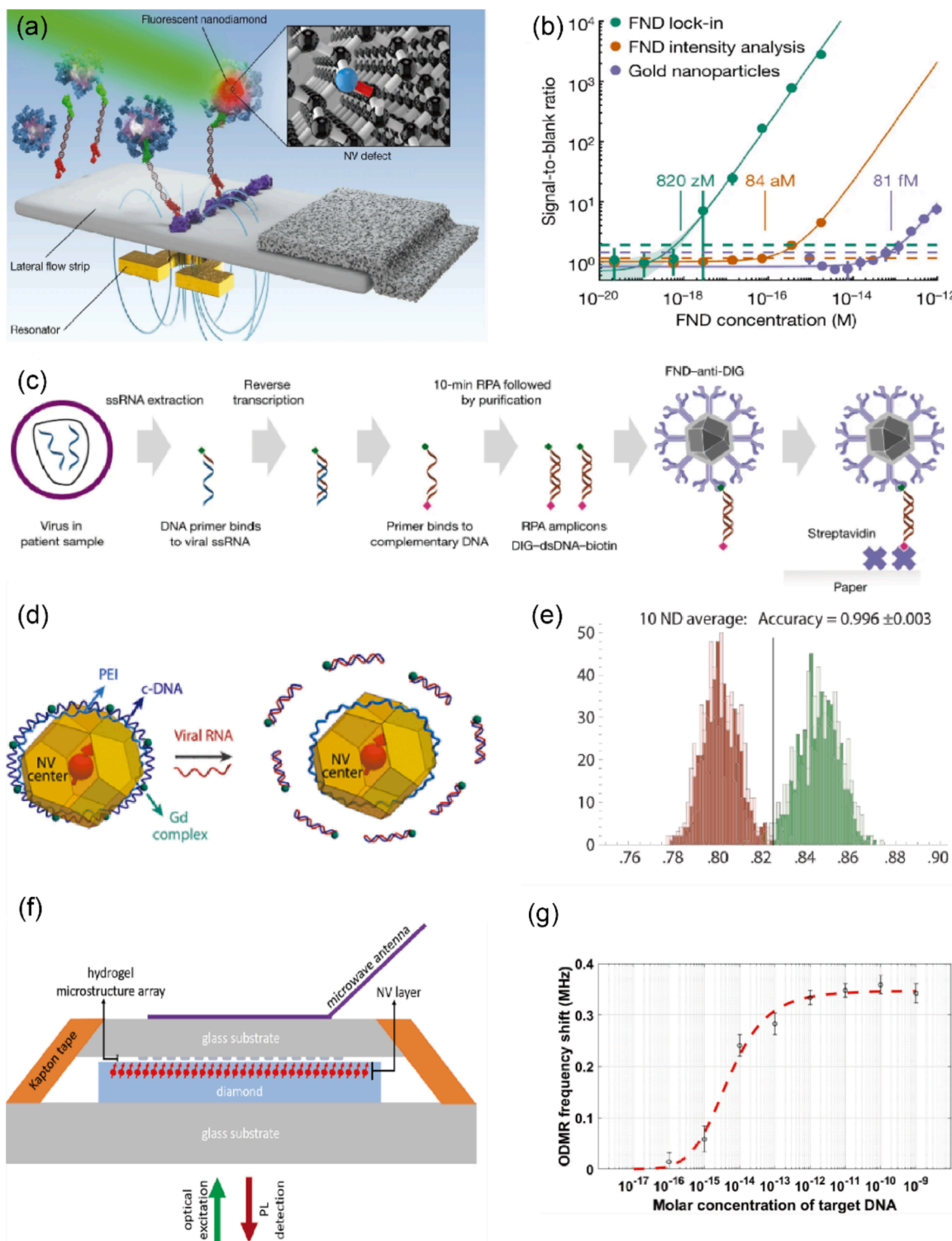


**Fig. 6.** Diamond-based sensor for measuring RNA and DNA. (a) Illustration of the concept of using FNDs in an LFA. The binding of DNA modifications causes NIDs to be immobilized at the test line in a sandwich-format LFA. The inset shows the atomic structure of an NV center. An omega-shaped strip line resonator applies a microwave field over the LFA, modulating the fluorescence intensity [37]. (b) Comparison of the detection limit for different detected methods in (a) [37]. (c) A schematic of the assay. Digoxigenin (DIG) and biotin-modified primers were used in a RT-RPA reaction to produce labelled amplicons, which bind to anti-DIG-functionalized FNDs and streptavidin-printed test lines on the LFA strips, forming a sandwich structure in the presence of amplicons. [37]. (d) Viral RNA detection with  $\text{Gd}^{3+}$  ions.  $\text{Gd}^{3+}$  complex molecules that can induce strong magnetic noise are connected to the c-DNA structure. In the presence of virus RNA, the base-pair matching of c-DNA and RNA leads to detachment of c-DNA-DOTA- $\text{Gd}^{3+}$  from the nanodiamond surface, resulting in weaker magnetic interaction between  $\text{Gd}^{3+}$  complex and NV centers inside the nanodiamond [91]. (e) Histogram of measured PL averaged from 10 NDs at a fixed dark time  $\tau = 200$ . The red (green) distribution corresponds to the case where viral RNA is absent (present) [91]. (f) DNA detection with microfluid step. Schematic illustration of the diamond-based sensor chip assembled for ODMR measurements [92]. (g) Maximum ODMR frequency shift in response to target DNA concentration [92].

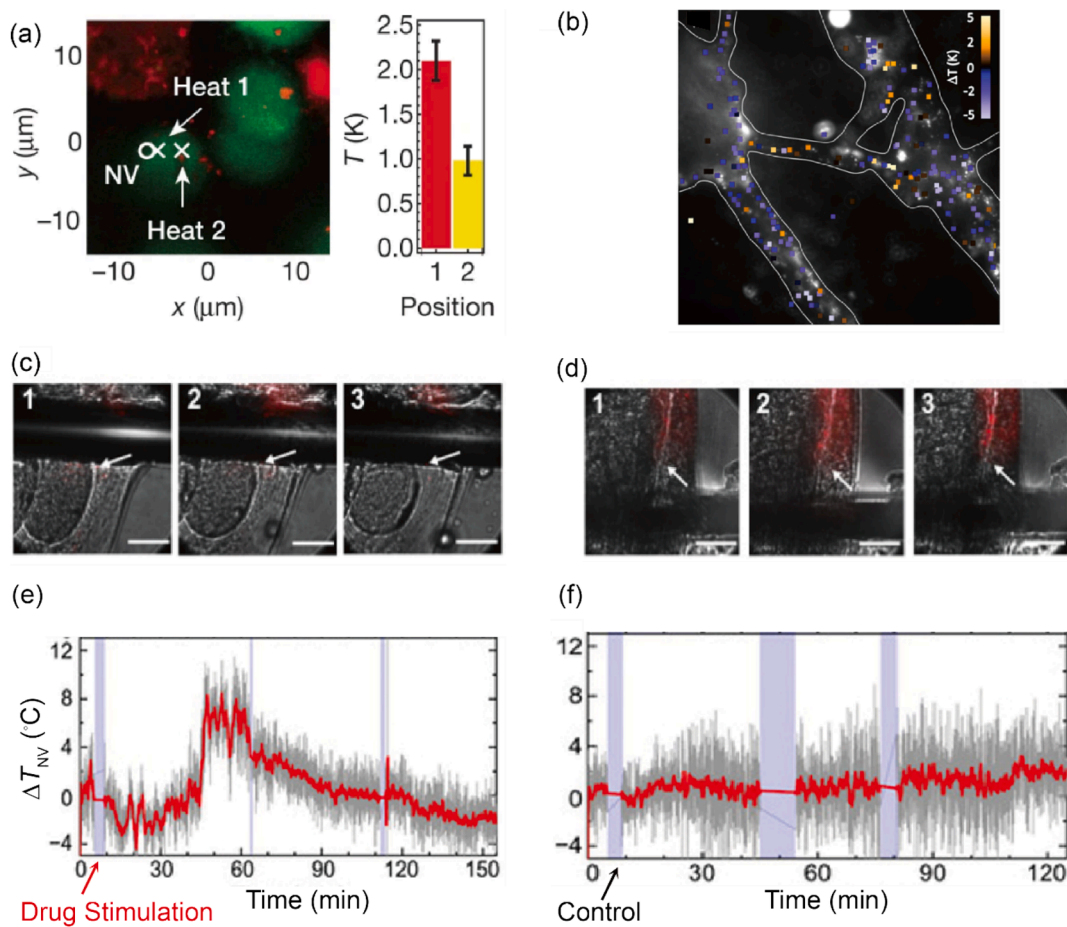


**Fig. 7.** Nanodiamond-based sensor for thermometry and its application (a) Single-position thermometry in living cells. Exogenous heating of stained human embryonic fibroblast WS1 cells, stained with calcine AM. Temperature of a single nanodiamond (circle in micrograph) with local heat applied at two different locations (crosses) is plotted (right) [104]. (b) Widefield temperature map from colocalized NDs overlaid with the ND fluorescence image of primary cortical neurons at 37.3 °C [39]. (c) Temperature monitor of worms under drug stimulation. (Top left and right) Merged fluorescence and bright field images of NDs during carbonyl cyanide p-trifluoromethoxyphenylhydrazone (FCCP) stimulation (60  $\mu$ M) and vehicle control experiments. The numbers indicate the timestamps of pictures captured during measurement indicated in lower left and right. (Lower left and right) Time profiles of  $\Delta T_{NV}$  during FCCP stimulation and vehicle control experiments. The blue shaded regions represent periods when no temperature measurement is performed. The photographs in Top left and right were obtained during these periods [106].

ODMR spectral shape and instrumental errors, enabling accurate real-time temperature measurement during dynamic thermal events [105]. They demonstrated *in vivo* real-time temperature monitoring inside *Caenorhabditis elegans* worms (Fig. 7c-f) [106]. Similarly, another group demonstrated the interplay between intracellular forces and the cytoplasmic rheology in live cells [107]. This advancement enables the direct identification of pharmacological thermogenesis, potentially allowing for the quantification of biological activities based on temperature.

Apart from biological applications, thermometry based on nanodiamonds with NV centers is still being refined. In an earlier study, dynamical decoupling protocols with newly designed spin pulse sequences facilitated selective thermal measurements and converted thermally induced shifts in the NV center's spin resonance frequencies into significant changes in its fluorescence, achieving higher sensitivities approaching 10 mK $\cdot$ Hz $^{-1/2}$  [108]. In a recent study, thermometry based on microwave-dressed spin states also provides selective sensitivity to temperature changes and can mitigate the influence of magnetic fields, thereby reducing measurement system errors [109]. Advances in thermal measurement technology enable accurate and rapid temperature measurements within cells.

In addition, nanodiamonds can be modified, such as into needle shapes [110], to meet various biological detection needs, especially by being hybridized with other functional materials. For example, in one

demonstration, nanodiamonds were coupled with magnetic nanoparticles, where temperature changes were converted into magnetic field variations near the Curie temperature, enhancing temperature sensitivity to 11 mK $\cdot$ Hz $^{-1/2}$  [111], and even 79  $\mu$ K $\cdot$ Hz $^{-1/2}$  [112]. Furthermore, nanodiamonds can be coupled with other nanoheater, such as gold nanorods [113], and polydopamine (PDA) [114], to serve as combined nanoheater/nanothermometer for researching nanoscale heat transfer and dissipation process. Studies have measured thermostability of cell membranes (Fig. 8a) [113], intracellular thermal conductivity (Fig. 8b) [114] and temperature gradient across locally heated *Caenorhabditis elegans* embryos [115]. Moreover, hybrid plasmonic nanodiamonds can be utilized as thermal agents for local photothermal therapy (PTT) against melanoma *in vivo* thermotherapeutic treatments (Fig. 8c) [116]. However, hybrid measurements can cause thermal damage to the sample. This damage can alter biological responses, compromise sample integrity, and affect the accuracy of subsequent measurements. To address this issue, researchers have opted for decoupled sensing [117], which involves using separate lasers for heating and sensing, to explore biological applications, like cell-cycle [115] more effectively.

Currently, nanodiamond thermometry techniques have demonstrated the impact of temperature on biological processes. Multi-parametric analysis can further enhance the accuracy of these thermometric measurements [118]. All-optical nanodiamond

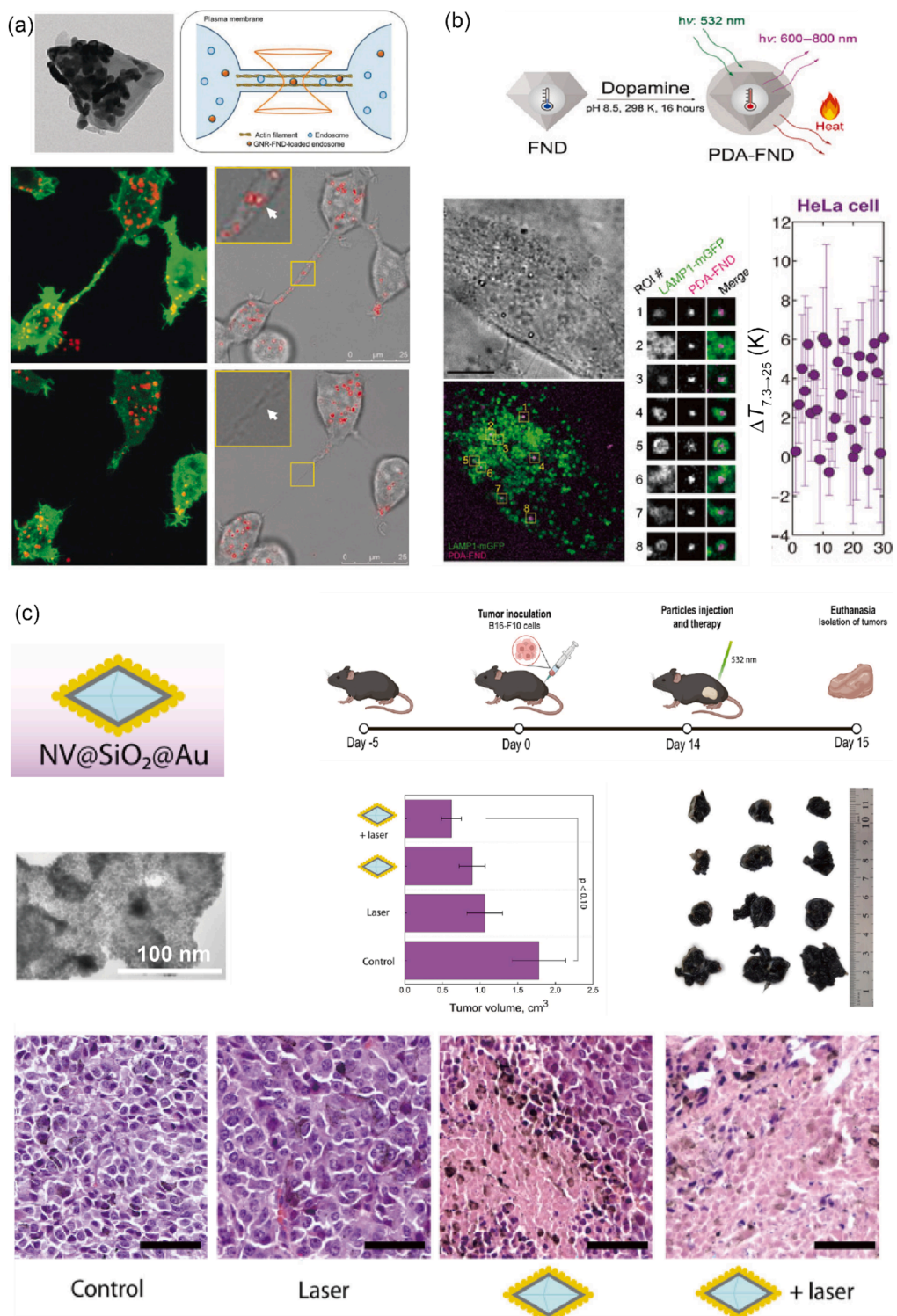


**Fig. 8.** Nanodiamond coupled with other nanoheater and its applications. (a) Hybrid gold nanorods and FNDs (GNR-FNDs) for nanohyperthermia in membrane nanotubes. The top left panel shows a TEM image of the hybrid structure. The top left panel shows a TEM image of the hybrid structure. The top right panel presents a schematic of the experiment using a laser beam for both heating and temperature sensing of the GNR-FNDs trapped in the endosomes of a membrane nanotube. The middle left panel displays fluorescence images, while the middle right panel shows merged bright-field/fluorescence images of HEK293T cells transduced with actin-GFP fusion proteins (green) and labeled with GNR-FNDs (red). The bottom left panel shows fluorescence images, and the bottom right panel presents merged bright-field/fluorescence images of the samples after exposure to a 594 nm laser with a power of 330 mW for 6 s [113]. (b) Hybrid functionalized PDA-FNDs for intracellular thermal conductivity measurement. The top panel illustrate PDA-FNDs prepared from FNDs. Confocal microscopy images (bottom left) of HeLa cells overexpressing LAMP1-mGFP that were incubated with PDA-FNDs for 4 h. Bottom right shows the temperature increase measured by FNDs in HeLa cells. The thermal conductivity is calculated through the average of temperature increase [114]. (c) Hybrid FND and gold nanoparticles for local PTT against melanoma in vivo. Top right is the scheme of therapy and tumor growth estimation. Middle shows the comparison of measured tumor volumes after PTT. (Bottom right) Digital photos of tumors extracted after the therapy. (Bottom) H&E-stained histological images of tumors after treatment with NV@SiO<sub>2</sub>@Au with laser, or NV@SiO<sub>2</sub>@Au, or control with laser, or control with 0.9% NaCl [116].

thermometry has been developed to extend the capabilities of current thermometry based on quantum spin. However, like other fluorescence-based thermometry methods, all-optical thermometry is susceptible to potential measurement errors induced by factors such as refractive index, viscosity, pH, and the presence of proteins. Advances in these techniques could unveil the mechanisms of thermal signaling by investigating the sensing and utilization of intracellular heat in physiological phenomena. The study of thermal biology, based on intracellular temperature variations detected by nanodiamond thermometers, holds the potential to significantly advance our understanding of the principles governing intracellular thermal dynamics in the near future.

#### 4. Nanodiamond-Based nanocarrier design and application for drug delivery

Nanodiamonds have emerged as excellent sensors for various biological activities within living cells. The performance of nanodiamonds is influenced not only by the spin properties of the NV center and the advancements in metrology but also by the intrinsic physical properties of the diamond itself as a functional carrier at the nanoscale. These factors significantly impact their efficacy in the phagocytosis efficiency of living cells and intracellular signal detection. For instance, factors such as morphology, topology, and surface chemistry must be carefully considered in the design of sensors before their use.

##### 4.1. Morphology control

Controlling nanodiamonds size and shape can optimize their use as nanocarriers for quantum sensing and other biological applications. Firstly, the size of nanodiamonds plays a significant role in their cellular uptake. Particles around 50 nm are most effective for internalization [119–123]. To achieve nanodiamonds of specific sizes, one common approach is detonation synthesis, which produces nanodiamonds through the explosion of carbon-containing materials [124]. This method is cost-effective and scalable but often results in a wide distribution of particle sizes. To address this issue, post-synthesis treatments such as high-temperature annealing and acid purification are employed to refine the morphology and surface chemistry of the nanodiamonds [125]. Another method involves chemical vapor deposition (CVD), which allows for precise control over the size of nanodiamonds by manipulating the growth parameters [43]. CVD-synthesized nanodiamonds typically exhibit well-defined morphologies, making them suitable for high-precision applications.

Additionally, surface morphology can influence the positioning of nanodiamonds within the cell upon uptake. Researchers have found that the circularity of the nanoparticles determines the ability of nanoparticles to escape membrane-bound vesicles during endocytosis. Specifically, nanoparticles with lower circularity (i.e., sharper nanoparticles) are more likely to escape [126,127]. For instance, prickly nanodiamonds exhibit rapid endosomal escape, allowing them to reside stably in the cytoplasm without significant cytotoxicity [41]. Thus, developing methods for controlling the morphology of nanodiamonds is essential for optimizing their performance in various applications. Common physical approaches, such as focused ion beam (FIB) techniques [128], offer high control over particle size and shape but can be limited by low yield and high production costs. Air oxidation, a chemical approach, is a promising method for achieving high yield and low cost [129]. This technique uses atmospheric oxygen to oxidize carbon atoms into carbon dioxide at elevated temperatures. Thermal oxidation method not only helps control the surface shape but also removes non-diamond impurities. This method has the potential to be more efficient, scalable, and cost-effective for precise morphology control.

The above mature nanodiamond shape engineering enable nanodiamonds as nanocarriers to meet various biological applications. This multifaceted approach to morphology control will pave the way for the development of more effective nanocarrier systems.

##### 4.2. Surface functionalization

The surface functionalization of nanodiamonds not only enhances their colloidal stability and biocompatibility but also expands their functionalities for a broader range of applications, thereby enhancing their potential as biosensors and drug carriers. Various functional groups can be introduced onto the surface of nanodiamonds through chemical reactions. For example, the chemical deaggregation method can produce single-digit detonation nanodiamonds (DNDs) while simultaneously introducing carboxyl groups [130]. By maintaining a high negative surface charge, nanodiamonds in suspension are stabilized and prevented from aggregating in biological environments. Additionally, the presence of carboxyl groups facilitates further chemical modifications, enabling the attachment of drugs or targeting ligands. Coating nanodiamonds with hydrophilic polymers or sugars, such as fructose, can also significantly enhance their solubility and prevent aggregation, thereby improving their effective cellular uptake [131]. Moreover, this approach allows for specific targeting of cancer cells, thereby achieving desired sensing and other applications.

Physical methods, such as sonication, can also be employed to enhance the functionalization of nanodiamonds. Shulevitz introduced a one-pot method for functionalizing milled nanodiamonds through emulsification, which allows for the formation of stable aqueous dispersions without complex chemical reactions [132]. This technique simplifies the functionalization process and can be adapted for various applications, including drug delivery and quantum sensing.

Thus, the surface functionalization of nanodiamonds is a vital process that enhances their potential as nanocarriers in biomedical applications. By employing various chemical and physical modification techniques, researchers can tailor the properties of nanodiamonds to improve their stability, targeting capabilities, and multifunctionality, paving the way for innovative therapeutic strategies.

##### 4.3. Drug delivery

Through the aforementioned surface functionalization and morphology control, these nanodiamonds can serve as suitable nanocarriers, enhancing their stability and biocompatibility. Due to these properties, nanodiamonds have been utilized in quantum sensing and drug delivery. While the use of nanodiamonds as quantum sensors has been previously described, we will now explore their application in drug delivery. The fluorescent property of the nanodiamonds can also be used for real-time monitoring of drug delivery and distribution within cells [133]. Nanodiamond-based drug delivery can be carried out in response to endogenous stimuli or exogenous stimuli.

Endogenous stimuli, such as overexpressed receptors and pH, enable selective targeting of tumor cells [134]. In an early study, nanodiamonds (NDs) were conjugated with transferrin-doxorubicin (Tf-DOX) complex to form ND-(Tf-DOX) nanodrug. Transferrin was conjugated to NDs so that the nanodrug could be selectively internalized into tumor cells with overexpressed transferrin receptors by transferrin receptor-mediated endocytosis. The fluorescence from NDs was used to identify the nanodrug in fluorescence images. Although the nanodrug inhibited tumor growth with less side effects compared to DOX alone, it still exhibited some toxic effects to the liver and spleen of mice [135]. In another study, NDs were coated with DOX-conjugated biopolymer to form DOX-NDs that exhibited lower toxicity. The acid-labile hydrazone linker between DOX and biopolymer can be cleaved at acidic environment in tumor tissue, enabling selective targeting of tumor cells by DOX-NDs. Thanks to the biocompatibility of the biopolymer, DOX-ND exhibited low cytotoxicity even at high concentrations. Furthermore, the intracellular distribution of DOX-NDs was examined by fluorescence spectra via *in vivo* experiments for breast cancer [136]. To diversify cancer therapies, ND-polyethylene glycol-hydrazine hydrate-folic acid complex was conjugated with DOX to form NPHF/D nanoparticles. The nanoparticles could selectively target tumor cells with overexpressed

folate receptors, displaying excellent therapeutic effects for breast, cervical, and liver cancer. The fluorescence from NDs was quenched in normal pH and recovered in low pH of tumor cells, making the nanoparticles an on-off imaging material [137].

Diverse exogenous stimuli, such as ultrasound, magnetic field [138], and light, can be employed for selective targeting of tumor cells [139]. For ultrasound-enhanced drug delivery with tissue penetrability and localized applicability, NDs were loaded with DOX and encapsulated by photoresist (PR) copolymer to form DOX-NDs/PR nanoparticles to which low-intensity focused ultrasound was applied for promoting intratumoral penetration of the nanoparticles, resulting in excellent antitumor effect [140]. For tissue-penetrative magnetic field-enhanced drug delivery, annealed magnetic nanodiamonds (MNDa), which were formed by the laser, chemical, and thermal treatment on the NDs, were conjugated with human serum albumin (HSA) and physically adsorbed to DOX to construct MNDa-HSA-DOX. Using external magnetic fields, tumor cells were selectively targeted. The fluorescence from MNDa was used to identify MNDa-HSA-DOX in fluorescence images [141]. For light-enhanced drug delivery with capability to be locally focused, NDs were conjugated with a locking strand (LS) to form LS-NDs. The photocleavable *ortho*-nitrobenzyl molecule linker between the LS and the ND could be cleaved upon ultraviolet light irradiation, enabling selective targeting of tumor cells [142].

## 5. Perspective

The field of nanodiamond-based sensing for biological applications has made remarkable strides, advancing from cellular to the molecular level detection with sensitivity surpassing many conventional technologies. Nanodiamonds stand out due to their biocompatibility, stability, and multifunctionality, making them ideal for both sensing and drug delivery.

Even with these advances, there are still many opportunities to explore in biological applications and fundamental research. In fundamental cellular research, nanodiamonds allow detailed studies of cellular metabolism and molecular dynamics. For example, using NV centers, they can detect molecules like ATP, deepening our understanding of cellular functions. In early disease diagnostics, they can identify early molecular markers of diseases such as cancer or neurodegenerative disorders, potentially leading to better patient outcomes. Additionally, integrating nanodiamond sensors into point-of-care devices, like lateral flow assays, could enable real-time monitoring of therapeutic responses, providing critical insights into drug efficacy and resistance.

While nanodiamonds hold immense promise for biological sensing, they face significant challenges that limit their full potential. Variability in properties such as size, shape, and nitrogen-vacancy (NV) center density leads to inconsistent performance, reducing measurement accuracy and reliability. Moreover, pulse-based techniques, despite their high sensitivity, are hindered in intracellular applications by the constant motion of nanodiamonds within cells, which disrupts signal acquisition. To overcome these drawbacks, standardized fabrication methods are essential to ensure uniform nanodiamond properties, thereby improving consistency and reliability. Additionally, developing advanced pulse sequences capable of tracking nanodiamonds in real time within living cells would enhance sensitivity and enable more effective live-cell applications. These advancements, driven by precision engineering and innovative measurement approaches, will set the stage for more robust and versatile nanodiamond-based technologies.

Physical and chemical modifications can further unlock the full potential of nanodiamonds in both sensing and drug delivery applications. Surface functionalization, achieved by attaching specific ligands or polymers to nanodiamond surfaces, enhances cellular uptake and specificity, enabling nanodiamonds to target particular cell types or organelles. This reduces interference from the complex intracellular environment, boosting sensing accuracy and improving the precision of

therapeutic payload delivery. Additionally, NV density optimization through techniques like electron beam or femtosecond laser writing produces brighter fluorescent nanodiamonds (FNDs), improving the signal-to-noise ratio (SNR) and measurement accuracy.

Looking ahead, miniaturization represents a key pathway to broaden the impact of nanodiamond technologies by enabling the development of advanced, compact systems with diverse applications. Through this process, researchers can create portable diagnostic devices—compact, user-friendly platforms that bring nanodiamond-based sensing to point-of-care settings, significantly speeding up diagnostics and enhancing accessibility. Additionally, implantable sensors made from miniaturized nanodiamonds could be integrated into the body, offering continuous monitoring of molecular signals and delivering real-time health insights. Furthermore, by pairing nanodiamonds with other nanomaterials, hybrid systems could emerge, capable of simultaneous sensing and therapeutic action, thus amplifying their utility across multiple domains. This ambitious push toward miniaturization hinges on interdisciplinary innovation, requiring the seamless integration of nanotechnology, physics, and biology to produce scalable, practical solutions that advance both research and healthcare.

Nanodiamond-based sensors stand as a groundbreaking technology with the power to transform biomedical science. Their unique properties enable molecular-level insights into disease and treatment, while their potential applications span diagnostics, therapy, and fundamental research. By addressing current limitations—such as variability and measurement challenges—through standardized fabrication and advanced techniques, and by enhancing the platform with physical and chemical methods, nanodiamonds can achieve greater precision and versatility. Furthermore, pursuing miniaturization will make these technologies widely accessible, from labs to clinics. As these strategies converge, nanodiamond sensors are poised to redefine our understanding of cellular processes and elevate the future of healthcare, offering new perspectives on the molecular dynamics of life.

## Declaration of Competing Interest

The authors declare that they have no known competing financial interests or personal relationships that could have appeared to influence the work reported in this paper.

## Acknowledgments

Z.Q.C. acknowledges the financial support from the National Natural Science Foundation of China (NSFC) and the Research Grants Council (RGC) of the Hong Kong Joint Research Scheme (Project No. N\_HKU750/23), HKU seed fund, and the Health@InnoHK program of the Innovation and Technology Commission of the Hong Kong SAR Government.

H.K. acknowledges the financial support from the National Research Foundation of Korea (NRF) grant funded by the Korean government (MSIT) (No. RS-2023-00208427), the Nano & Material Technology Development Program through the National Research Foundation of Korea (NRF) funded by Ministry of Science and ICT (RS-2024-00407234) and a Korea University Grant.

## Data availability

No data was used for the research described in the article.

## References

- [1] F. Fröhlich, M. Bazhenov, V. Iragui-Madoz, T.J. Sejnowski, Potassium dynamics in the epileptic cortex: new insights on an old topic, *Neuroscientist* 14 (2008) 422–433.
- [2] Y. Li, W. Maret, Transient fluctuations of intracellular zinc ions in cell proliferation, *Exp. Cell Res.* 315 (2009) 2463–2470.

[3] Y. Li, B.E. Hawkins, D.S. DeWitt, D.S. Prough, W. Maret, The relationship between transient zinc ion fluctuations and redox signaling in the pathways of secondary cellular injury: relevance to traumatic brain injury, *Brain Res.* 1330 (2010) 131–141.

[4] M. Guragain, D.L. Lenaburg, F.S. Moore, I. Reutlinger, M.A. Patrauchan, Calcium homeostasis in *Pseudomonas aeruginosa* requires multiple transporters and modulates swarming motility, *Cell Calcium* 54 (2013) 350–361.

[5] G.N. Bruni, R.A. Weekley, B.J. Dodd, J.M. Kralj, Voltage-gated calcium flux mediates *Escherichia coli* mechanosensation, *Proc. Natl. Acad. Sci.* 114 (2017) 9445–9450.

[6] M.V. Accardi, B.A. Daniels, P.M. Brown, J.-M. Fritschy, S.K. Tyagarajan, D. Bowie, Mitochondrial reactive oxygen species regulate the strength of inhibitory GABA-mediated synaptic transmission, *Nat. Commun.* 5 (2014) 3168.

[7] E. Stanganello, A.I. Hagemann, B. Mattes, C. Sinner, D. Meyen, S. Weber, A. Schug, E. Raz, S. Scholpp, Filopodia-based Wnt transport during vertebrate tissue patterning, *Nat. Commun.* 6 (2015) 5846.

[8] C. Kim, N. Kang, S. Min, R. Thangam, S. Lee, H. Hong, K. Kim, S.Y. Kim, D. Kim, H. Rha, K.-R. Tag, H.-J. Lee, N. Singh, D. Jeong, J. Hwang, Y. Kim, S. Park, H. Lee, T. Kim, S.W. Son, S. Park, S. Karamikamkar, Y. Zhu, A. Hassani Najafabadi, Z. Chu, W. Sun, P. Zhao, K. Zhang, L. Bian, H.-C. Song, S.-G. Park, J.S. Kim, S.-Y. Lee, J.-P. Ahn, H.-K. Kim, Y.S. Zhang, H. Kang, Modularity-based mathematical modeling of ligand inter-nanocluster connectivity for unraveling reversible stem cell regulation, *Nat. Commun.* 15 (2024) 10665.

[9] M. Stocker, Ca<sup>2+</sup>-activated K<sup>+</sup> channels: molecular determinants and function of the SK family, *Nat. Rev. Neurosci.* 5 (2004) 758–770.

[10] T.H. Sleutels, A. ter Heijne, P. Kuntke, C.J. Buisman, H.V. Hamelers, Membrane selectivity determines energetic losses for ion transport in bioelectrochemical systems, *ChemistrySelect* 2 (2017) 3462–3470.

[11] K. Okabe, N. Inada, C. Gota, Y. Harada, T. Funatsu, S. Uchiyama, Intracellular temperature mapping with a fluorescent polymeric thermometer and fluorescence lifetime imaging microscopy, *Nat. Commun.* 3 (2012) 705.

[12] D. Chretien, P. Bénit, H.-H. Ha, S. Keiper, R. El-Khoury, Y.-T. Chang, M. Jastroch, H.T. Jacobs, P. Rustin, M. Rak, Mitochondria are physiologically maintained at close to 50 °C, *PLoS Biol.* 16 (2018) e2003992.

[13] H. Bunch, B.P. Lawney, Y.-F. Lin, A. Asaithamby, A. Murshid, Y.E. Wang, B. P. Chen, S.K. Calderwood, Transcriptional elongation requires DNA break-induced signalling, *Nat. Commun.* 6 (2015) 10191.

[14] M. Tresini, D.O. Warmerdam, P. Kolovos, L. Snijder, M.G. Vrouwe, J.A. Demmers, W.F. Van Ijcken, F.G. Grosveld, R.H. Medema, J.H. Hoeijmakers, The core spliceosome as target and effector of non-canonical ATM signalling, *Nature* 523 (2015) 53–58.

[15] C.K. Glass, G. Natoli, Molecular control of activation and priming in macrophages, *Nat. Immunol.* 17 (2016) 26–33.

[16] S. Lee, J. Yoo, G. Bae, R. Thangam, J. Heo, J.Y. Park, H. Choi, C. Kim, J. An, J. Kim, K.R. Mun, S. Shin, K. Zhang, P. Zhao, Y. Kim, N. Kang, S.-B. Han, D. Kim, J. Yoon, M. Kang, J. Kim, L. Yang, S. Karamikamkar, J. Kim, Y. Zhu, A. H. Najafabadi, G. Song, D.-H. Kim, K.-B. Lee, S.J. Oh, H.-D. Jung, H.-C. Song, W. Y. Jang, L. Bian, Z. Chu, J. Yoon, J.S. Kim, Y.S. Zhang, Y. Kim, H.S. Jang, S. Kim, H. Kang, Photonic control of ligand nanoscaping in self-assembly regulates stem cell fate, *Bioact. Mater.* 34 (2024) 164–180.

[17] K.C. Hart, J. Tan, K.A. Siemers, J.Y. Sim, B.L. Pruitt, W.J. Nelson, M. Gloerich, E-cadherin and LGN align epithelial cell divisions with tissue tension independently of cell shape, *Proc. Natl. Acad. Sci.* 114 (2017) E5845–E5853.

[18] X. Luo, L. Guo, L. Zhang, Y. Hu, D. Shang, D. Ji, Bioinformatics analysis of microarray profiling identifies the mechanism of focal adhesion kinase signalling pathway in proliferation and apoptosis of breast cancer cells modulated by green tea polyphenol epigallocatechin 3-gallate, *J. Pharm. Pharmacol.* 70 (2018) 1606–1618.

[19] W.-J. Pannekoek, J. De Rooij, M. Gloerich, Force Transduction by Cadherin Adhesions in Morphogenesis F1000Research (2019) 8.

[20] C.G. Vasquez, A.C. Martin, Force transmission in epithelial tissues, *Dev. Dyn.* 245 (2016) 361–371.

[21] X. Zhao, J.-L. Guan, Focal adhesion kinase and its signaling pathways in cell migration and angiogenesis, *Adv. Drug Deliv. Rev.* 63 (2011) 610–615.

[22] Y. El-Gohary, S. Tulachan, P. Guo, C. Welsh, J. Wiersch, K. Prasad, J. Paredes, C. Shiota, X. Xiao, Y. Wada, Smad signaling pathways regulate pancreatic endocrine development, *Dev. Biol.* 378 (2013) 83–93.

[23] C. Sanchez-Jimenez, J.M. Izquierdo, T-cell intracellular antigen (TIA)-proteins deficiency in murine embryonic fibroblasts alters cell cycle progression and induces autophagy, *PLoS One* 8 (2013) e75127.

[24] C.F. Bentzinger, Y.X. Wang, M.A. Rudnicki, Building muscle: molecular regulation of myogenesis, *Cold Spring Harb. Perspect. Biol.* 4 (2012) a008342.

[25] F. Hu, N. Li, Z. Li, C. Zhang, Y. Yue, Q. Liu, L. Chen, P.J. Bilan, W. Niu, Electrical pulse stimulation induces GLUT4 translocation in a Rac-Akt-dependent manner in C2C12 myotubes, *FEBS Lett.* 592 (2018) 644–654.

[26] Y. Guan, X. Shan, F. Zhang, S. Wang, H.-Y. Chen, N. Tao, Kinetics of small molecule interactions with membrane proteins in single cells measured with mechanical amplification, *Sci. Adv.* 1 (2015) e1500633.

[27] K. Wang, Z. Cao, Q. Ding, J. Yoo, N. Singh, H. Kang, L. Wang, L. Xu, J.S. Kim, Electronic structure tuning of layered double hydroxides for electrochemical sensing and its biomedical applications, *Sci. China Chem.* 67 (2024) 3614–3630.

[28] W. Wang, Y. Yang, S. Wang, V.J. Nagaraj, Q. Liu, J. Wu, N. Tao, Label-free measuring and mapping of binding kinetics of membrane proteins in single living cells, *Nat. Chem.* 4 (2012) 846–853.

[29] N. Yu, J.M. Atienza, J. Bernard, S. Blanc, J. Zhu, X. Wang, X. Xu, Y.A. Abassi, Real-Time Monitoring of Morphological Changes in Living Cells by Electronic Cell Sensor Arrays: An Approach To Study G Protein-Coupled Receptors, *Anal. Chem.* 78 (2006) 35–43.

[30] A. Orte, J.M. Alvarez-Pez, M.J. Ruedas-Rama, Fluorescence Lifetime Imaging Microscopy for the Detection of Intracellular pH with Quantum Dot Nanosensors, *ACS Nano* 7 (2013) 6387–6395.

[31] D. Le Sage, K. Arai, D.R. Glenn, S.J. DeVience, L.M. Pham, L. Rahn-Lee, M. D. Lukin, A. Yacoby, A. Komeili, R.L. Walsworth, Optical magnetic imaging of living cells, *Nature* 496 (2013) 486–489.

[32] H. Hong, S. Min, S. Koo, Y. Lee, J. Yoon, W.Y. Jang, N. Kang, R. Thangam, H. Choi, H.J. Jung, S.B. Han, Q. Wei, S.H. Yu, D.H. Kim, R. Paulmurugan, W. K. Jeong, K.B. Lee, T. Hyeon, D. Kim, H. Kang, Dynamic Ligand Screening by Magnetic Nanoassembly Modulates Stem Cell Differentiation, *Adv Mater* 34 (2022) e2105460.

[33] Y. Kim, R. Thangam, J. Yoo, J. Heo, J.Y. Park, N. Kang, S. Lee, J. Yoon, K.R. Mun, M. Kang, Photoswitchable Microgels for dynamic macrophage modulation, *Adv. Mater.* 34 (2022) 2205498.

[34] F. Perona Martinez, A.C. Nusantara, M. Chipaux, S.K. Padamati, R. Schirhagl, Nanodiamond Relaxometry-Based Detection of Free-Radical Species When Produced in Chemical Reactions in Biologically Relevant Conditions, *ACS Sensors* 5 (2020) 3862–3869.

[35] J.-K. Choi, J. Lee, Membrane-based chemomechanical transducer for the detection of aptamer-protein binding, in: 2015 28th IEEE International Conference on Micro Electro Mechanical Systems (MEMS), 2015, pp. 219–222.

[36] S.K. Sarkar, A. Bumb, X. Wu, K.A. Sochaiki, P. Kellman, M.W. Brechbuhl, K. C. Neuman, Wide-field in vivo background free imaging by selective magnetic modulation of nanodiamond fluorescence, *Biomed. Opt. Express* 5 (2014) 1190–1202.

[37] B.S. Miller, L. Bezinge, H.D. Gliddon, D. Huang, G. Dold, E.R. Gray, J. Heaney, P. J. Dobson, E. Nastouli, J.J.L. Morton, R.A. McKendry, Spin-enhanced nanodiamond biosensing for ultrasensitive diagnostics, *Nature* 587 (2020) 588–593.

[38] M.W. Doherty, N.B. Manson, P. Delaney, F. Jelezko, J. Wrachtrup, L. C. Hollenberg, The nitrogen-vacancy colour centre in diamond, *Phys. Rep.* 528 (2013) 1–45.

[39] D.A. Simpson, E. Morrisroe, J.M. McCoey, A.H. Lombard, D.C. Mendis, F. Treussart, L.T. Hall, S. Petrou, L.C.L. Hollenberg, Non-Neurotoxic Nanodiamond Probes for Intraneuronal Temperature Mapping, *ACS Nano* 11 (2017) 12077–12086.

[40] H.C. Davis, P. Ramesh, A. Bhatnagar, A. Lee-Gosselin, J.F. Barry, D.R. Glenn, R. L. Walsworth, M.G. Shapiro, Mapping the microscale origins of magnetic resonance image contrast with subcellular diamond magnetometry, *Nat. Commun.* 9 (2018) 131.

[41] Z. Chu, K. Miu, P. Lung, S. Zhang, S. Zhao, H.-C. Chang, G. Lin, Q. Li, Rapid endosomal escape of prickly nanodiamonds: implications for gene delivery, *Sci. Rep.* 5 (2015) 11661.

[42] C.J.H. Worts, R.S. Balmer, Diamond as an electronic material, *Mater. Today* 11 (2008) 22–28.

[43] T. Zhang, M. Gupta, J. Jing, Z. Wang, X. Guo, Y. Zhu, Y.C. Yiu, T.K.C. Hui, Q. Wang, K.H. Li, Z. Chu, High-quality diamond microparticles containing SiV centers grown by chemical vapor deposition with preselected seeds, *J. Mater. Chem. C* 10 (2022) 13734–13740.

[44] S. Li, J.-P. Chou, J. Wei, M. Sun, A. Hu, A. Gali, Oxygenated (113) diamond surface for nitrogen-vacancy quantum sensors with preferential alignment and long coherence time from first principles, *Carbon* 145 (2019) 273–280.

[45] P. Reineck, A. Francis, A. Orth, D.W.M. Lau, R.D.V. Nixon-Luke, I.D. Rastogi, W. A.W. Razali, N.M. Cordina, L.M. Parker, V.K.A. Sreenivasan, Brightness and Photostability of Emerging Red and Near-IR Fluorescent Nanomaterials for Bioimaging, *Adv. Opt. Mater.* 4 (2016) 1549–1557.

[46] F. Pedraza-Montero, K. Santacruz-Gómez, M. Acosta-Elías, E. Silva-Campa, D. Meza-Figueroa, D. Soto-Puebla, B. Castaneda, E. Urrutia-Bañuelos, O. Álvarez-Bajo, S. Navarro-Espinoza, Thermometric characterization of fluorescent nanodiamonds suitable for biomedical applications, *Appl. Sci.* 11 (2021) 4065.

[47] G. Davies, M. Hamer, Optical studies of the 1.945 eV vibronic band in diamond, *Proceedings of the Royal Society of London. A. Mathematical and Physical Sciences*, 348 (1976) 285–298.

[48] R. Epstein, F. Mendoza, Y. Kato, D. Awschalom, Anisotropic interactions of a single spin and dark-spin spectroscopy in diamond, *Nat. Phys.* 1 (2005) 94–98.

[49] T.P.M. Alegre, C. Santori, G. Medeiros-Ribeiro, R.G. Beausoleil, Polarization-selective excitation of nitrogen vacancy centers in diamond, *Physical Review B—Condensed Matter and Materials Physics* 76 (2007) 165205.

[50] M.N. Ashfold, J.P. Goss, B.L. Green, P.W. May, M.E. Newton, C.V. Peaker, Nitrogen in diamond, *Chem. Rev.* 120 (2020) 5745–5794.

[51] P.J. Scheidegger, S. Diesch, M.L. Palm, C.L. Degen, Scanning nitrogen-vacancy magnetometry down to 350 mK, *Appl. Phys. Lett.* 120 (2022).

[52] G.-Q. Liu, X. Feng, N. Wang, Q. Li, R.-B. Liu, Coherent quantum control of nitrogen-vacancy center spins near 1000 kelvin, *Nat. Commun.* 10 (2019) 1344.

[53] S. Phan, C.K. Luscombe, Recent trends in marine microplastic modeling and machine learning tools: Potential for long-term microplastic monitoring, *J. Appl. Phys.* 133 (2023).

[54] D.B. Bucher, D.P.L. Aude Craik, M.P. Backlund, M.J. Turner, O. Ben Dor, D. R. Glenn, R.L. Walsworth, Quantum diamond spectrometer for nanoscale NMR and ESR spectroscopy, *Nat. Protoc.* 14 (2019) 2707–2747.

[55] A. Mzyk, A. Sigaeva, R. Schirhagl, Relaxometry with Nitrogen Vacancy (NV) Centers in Diamond, *Acc. Chem. Res.* 55 (2022) 3572–3580.

[56] E. Bauch, S. Singh, J. Lee, C.A. Hart, J.M. Schloss, M.J. Turner, J.F. Barry, L. M. Pham, N. Bar-Gill, S.F. Yelin, R.L. Walsworth, Decoherence of ensembles of nitrogen-vacancy centers in diamond, *Phys. Rev. B* 102 (2020) 134210.

[57] P. Hemmer, C. Gomes, Single proteins under a diamond spotlight, *Science* 347 (2015) 1072–1073.

[58] Y. Kim, T.M. Koo, R. Thangam, M.S. Kim, W.Y. Jang, N. Kang, S. Min, S.Y. Kim, L. Yang, H. Hong, Submolecular ligand size and spacing for cell adhesion, *Adv. Mater.* 34 (2022) 2110340.

[59] G. Bae, M.S. Kim, R. Thangam, T.M. Koo, W.Y. Jang, J. Yoon, S.B. Han, L. Yang, S. Y. Kim, N. Kang, Receptor-Level Proximity and Fastening of Ligands Modulates Stem Cell Differentiation, *Adv. Funct. Mater.* 32 (2022) 2200828.

[60] Y. Tan, A. Tajik, J. Chen, Q. Jia, F. Chowdhury, L. Wang, J. Chen, S. Zhang, Y. Hong, H. Yi, Matrix softness regulates plasticity of tumour-repopulating cells via H3K9 demethylation and Sox2 expression, *Nat. Commun.* 5 (2014) 4619.

[61] R. Thangam, S.Y. Kim, N. Kang, H. Hong, H.J. Lee, S. Lee, D. Jeong, K.R. Tag, K. Kim, Y. Zhu, Ligand coupling and decoupling modulates stem cell fate, *Adv. Funct. Mater.* 33 (2023) 2206673.

[62] M. Li, L. Liu, N. Xi, Y. Wang, X. Xiao, W. Zhang, Nanoscale imaging and mechanical analysis of Fc receptor-mediated macrophage phagocytosis against cancer cells, *Langmuir* 30 (2014) 1609–1621.

[63] M.J. Ko, H. Hong, H. Choi, H. Kang, D.H. Kim, Multifunctional magnetic nanoparticles for dynamic imaging and therapy, *Adv. NanoBiomed Res.* 2 (2022) 2200053.

[64] R. Wang, Y.T. Chow, S. Chen, D. Ma, T. Luo, Y. Tan, D. Sun, Magnetic force-driven *in situ* selective intracellular delivery, *Sci. Rep.* 8 (2018) 14205.

[65] H. Lee, G. Han, Y. Na, M. Kang, S.-J. Bang, H.S. Kang, T.-S. Jang, J.-H. Park, H. L. Jang, K. Yang, H. Kang, H.-D. Jung, 3D-Printed Tissue-Specific Nanospike-Based Adhesive Materials for Time-Regulated Synergistic Tumor Therapy and Tissue Regeneration In Vivo, *Adv. Funct. Mater.* 34 (2024) 2406237.

[66] F. Xu, S. Zhang, L. Ma, Y. Hou, J. Li, A. Denisenko, Z. Li, J. Spatz, J. Wrachtrup, H. Lei, Quantum-enhanced diamond molecular tension microscopy for quantifying cellular forces, *Sci. Adv.* 10 (2024) eadi5300.

[67] L. Wang, Y. Hou, T. Zhang, X. Wei, Y. Zhou, D. Lei, Q. Wei, Y. Lin, Z. Chu, All-Optical Modulation of Single Defects in Nanodiamonds: Revealing Rotational and Translational Motions in Cell Traction Force Fields, *Nano Lett.* 22 (2022) 7714–7723.

[68] M.J. Ko, S. Min, H. Hong, W. Yoo, J. Joo, Y.S. Zhang, H. Kang, D.-H. Kim, Magnetic nanoparticles for ferroptosis cancer therapy with diagnostic imaging, *Bioact. Mater.* 32 (2024) 66–97.

[69] M. Katerji, M. Filippova, P. Duerksen-Hughes, Approaches and Methods to Measure Oxidative Stress in Clinical Samples: Research Applications in the Cancer Field, *Oxid. Med. Cell. Longev.* 2019 (2019) 1279250.

[70] K. Wu, Q. Lu, M. Sow, P. Balasubramanian, F. Jelezko, T. Weil, Y. Wu, Nanoscale detection and real-time monitoring of free radicals in a single living cell under the stimulation of targeting moieties using a nanodiamond quantum sensor, *Funct. Diamond* 4 (2024) 2336524.

[71] L. Nie, A.C. Nusantara, V.G. Damle, M.V. Baranov, M. Chipaux, C. Reyes-San-Martin, T. Hamoh, C.P. Epperla, M. Guricova, P. Cigler, G. van den Bogaart, R. Schirhagl, Quantum Sensing of Free Radicals in Primary Human Dendritic Cells, *Nano Lett.* 22 (2022) 1818–1825.

[72] S. Fan, H. Gao, Y. Zhang, L. Nie, R. Bartolo, R. Bron, H.A. Santos, R. Schirhagl, Quantum Sensing of Free Radical Generation in Mitochondria of Single Heart Muscle Cells during Hypoxia and Reoxygenation, *ACS Nano* 18 (2024) 2982–2991.

[73] S. Fan, L. Lopez Llorens, F.P. Perona Martinez, R. Schirhagl, Quantum Sensing of Free Radical Generation in Mitochondria of Human Keratinocytes during UVB Exposure, *ACS Sensors* 9 (2024) 2440–2446.

[74] Y. Zhang, A. Sigaeva, S. Fan, N. Norouzi, X. Zheng, I.H. Heijink, D.J. Slebos, S. D. Pouwels, R. Schirhagl, Dynamics for High-Sensitivity Detection of Free Radicals in Primary Bronchial Epithelial Cells upon Stimulation with Cigarette Smoke Extract, *Nano Lett.* 24 (2024) 9650–9657.

[75] H. Xu, D. Kim, Y.Y. Zhao, C. Kim, G. Song, Q. Hu, H. Kang, J. Yoon, Remote Control of Energy Transformation-Based Cancer Imaging and Therapy, *Adv. Mater.* 2402806 (2024).

[76] C. Reyes-San-Martin, A. Elías-Llumbet, E. Escobar-Chaves, M. Manterola, A. Mzyk, R. Schirhagl, Diamond-based quantum sensing of free radicals in migrating human breast cancer cells, *Carbon* 228 (2024) 119405.

[77] S. Fan, L. Nie, Y. Zhang, E. Ustyantseva, W. Woudstra, H. Kampinga, R. Schirhagl, Diamond quantum sensing revealing the relation between free radicals and huntington's disease, *ACS Cent. Sci.* 9 (2023) 1427–1436.

[78] K. Wu, T.A. Vedelaar, V.G. Damle, A. Morita, J. Mougnaud, C.R. San Martin, Y. Zhang, D.P. van der Pol, H. Ende-Metselaar, I. Rodenhuus-Zybert, Applying NV center-based quantum sensing to study intracellular free radical response upon viral infections, *Redox Biol.* 52 (2022) 102279.

[79] K. Wu, L. Nie, A.C. Nusantara, W. Woudstra, T. Vedelaar, A. Sigaeva, R. Schirhagl, Diamond Relaxometry as a Tool to Investigate the Free Radical Dialogue between Macrophages and Bacteria, *ACS Nano* 17 (2023) 1100–1111.

[80] A. Elias-Llumbet, Y. Tian, C. Reyes-San-Martin, A. Reina-Mahecha, V. Damle, A. Morita, H.C. van der Veen, P.K. Sharma, M. Sandovici, A. Mzyk, Quantum sensing for real-time monitoring of drug efficacy in synovial fluid from arthritis patients, *Nano Lett.* 23 (2023) 8406–8410.

[81] Y. Tian, A.C. Nusantara, T. Hamoh, A. Mzyk, X. Tian, F. Perona Martinez, R. Li, H. P. Permentier, R. Schirhagl, Functionalized fluorescent nanodiamonds for simultaneous drug delivery and quantum sensing in HeLa cells, *ACS Appl. Mater. Interfaces* 14 (2022) 39265–39273.

[82] J. Shin, N. Kang, B. Kim, H. Hong, L. Yu, J. Kim, H. Kang, J.S. Kim, One-dimensional nanomaterials for cancer therapy and diagnosis, *Chem. Soc. Rev.* 52 (2023) 4488–4514.

[83] I. Nazir, H.Z. Mahmood, S. Mustafa, Polymerase chain reaction: a creative review, *Journal of Applied. Biotechnol. Bioeng.* 7 (2020) 157–159.

[84] P. Rådström, R. Knutsson, P. Wolffs, M. Lövenklev, C. Löfström, Pre-PCR processing: strategies to generate PCR-compatible samples, *Mol. Biotechnol.* 26 (2004) 133–146.

[85] A. Patel, Initial public health response and interim clinical guidance for the 2019 novel coronavirus outbreak—United States, December 31, 2019–February 4, 2020, *MMWR Morb. Mortal. Wkly. Rep.* 69 (2020).

[86] B. Kaltenboeck, C. Wang, Advances in real-time PCR: Application to clinical laboratory diagnostics, *Adv. Clin. Chem.* 40 (2006) 219.

[87] J. Martin, How has the COVID-19 Pandemic Impacted PCR? *Biotechniques* 69 (2020) 1–3.

[88] M.B. Kulkarni, S. Goel, Advances in continuous-flow based microfluidic PCR devices—A review, *Eng. Res. Express* 2 (2020) 042001.

[89] J. Peter, G. Theron, D. Chanda, P. Clowes, A. Rachow, M. Lesosky, M. Hoelscher, P. Mwaba, A. Pym, K. Dheda, Test characteristics and potential impact of the urine LAM lateral flow assay in HIV-infected outpatients under investigation for TB and able to self-expectorate sputum for diagnostic testing, *BMC Infect. Dis.* 15 (2015) 1–12.

[90] J.I. García, H.V. Kelley, J. Meléndez, R.A.A. de León, A. Castillo, S. Sidiki, K. A. Yusof, E. Nunes, C.L. Téllez, C.R. Mejía-Villatoro, Improved Alere Determine Lipoparabinomannan Antigen Detection Test for the diagnosis of human and bovine tuberculosis by manipulating urine and milk, *Sci. Rep.* 9 (2019) 18012.

[91] C. Li, R. Soleyman, M. Kohandel, P. Cappellaro, SARS-CoV-2 Quantum Sensor Based on Nitrogen-Vacancy Centers in Diamond, *Nano Lett.* 22 (2022) 43–49.

[92] M. Kayci, J. Fan, O. Bakirman, A. Herrmann, Multiplexed sensing of biomolecules with optically detected magnetic resonance of nitrogen-vacancy centers in diamond, *Proc. Natl. Acad. Sci.* 118 (2021) e2112664118.

[93] J. Holzgrafe, Q. Gu, J. Beitner, D.M. Kara, H.S. Knowles, M. Atatüre, Nanoscale nmr spectroscopy using nanodiamond quantum sensors, *Phys. Rev. Appl* 13 (2020) 044004.

[94] F. Shi, F. Kong, P. Zhao, X. Zhang, M. Chen, S. Chen, Q. Zhang, M. Wang, X. Ye, Z. Wang, Single-DNA electron spin resonance spectroscopy in aqueous solutions, *Nat. Methods* 15 (2018) 697–699.

[95] I. Lovchinsky, A. Sushkov, E. Urbach, N.P. de Leon, S. Choi, K. De Greve, R. Evans, R. Gertner, E. Bersin, C. Müller, Nuclear magnetic resonance detection and spectroscopy of single proteins using quantum logic, *Science* 351 (2016) 836–841.

[96] T. Grousl, P. Ivanov, I. Frydlová, P. Vasicová, F. Janda, J. Vojtová, K. Malinska, I. Malcová, L. Nováková, D. Janosková, Robust heat shock induces eIF2α-phosphorylation-independent assembly of stress granules containing eIF3 and 40S ribosomal subunits in budding yeast, *Saccharomyces cerevisiae*, *J. Cell Sci.* 122 (2009) 2078–2088.

[97] K. Richter, M. Haslbeck, J. Buchner, The heat shock response: life on the verge of death, *Mol. Cell* 40 (2010) 253–266.

[98] C. Montell, M.J. Caterina, Thermoregulation: channels that are cool to the core, *Curr. Biol.* 17 (2007) R885–R887.

[99] T. Voets, K. Talavera, G. Owsianik, B. Nilius, Sensing with TRP channels, *Nat. Chem. Biol.* 1 (2005) 85–92.

[100] K.-I. Takeuchi, Y. Nakano, U. Kato, M. Kaneda, M. Aizu, W. Awano, S. Yonemura, S. Kiyonaka, Y. Mori, D. Yamamoto, Changes in temperature preferences and energy homeostasis in dystroglycan mutants, *Science* 323 (2009) 1740–1743.

[101] G. Baffou, H. Rignault, D. Marguet, L. Jullien, A critique of methods for temperature imaging in single cells, *Nat. Methods* 11 (2014) 899–901.

[102] S.-J. Yu, M.-W. Kang, H.-C. Chang, K.-M. Chen, Y.-C. Yu, Bright fluorescent nanodiamonds: no photobleaching and low cytotoxicity, *J. Am. Chem. Soc.* 127 (2005) 17604–17605.

[103] O.A. Shenderova, G.E. McGuire, Science and engineering of nanodiamond particle surfaces for biological applications, *Biointerphases* 10 (2015).

[104] G. Kucsko, P.C. Maurer, N.Y. Yao, M. Kubo, H.J. Noh, P.K. Lo, H. Park, M. D. Lukin, Nanometre-scale thermometry in a living cell, *Nature* 500 (2013) 54–58.

[105] M. Fujiwara, A. Dohms, K. Suto, Y. Nishimura, K. Oshimi, Y. Teki, K. Cai, O. Benson, Y. Shikano, Real-time estimation of the optically detected magnetic resonance shift in diamond quantum thermometry toward biological applications, *Phys. Rev. Res.* 2 (2020) 043415.

[106] M. Fujiwara, S. Sun, A. Dohms, Y. Nishimura, K. Suto, Y. Takezawa, K. Oshimi, L. Zhao, N. Sadzak, Y. Umehara, Real-time nanodiamond thermometry probing in vivo thermogenic responses, *Sci. Adv.* 6 (2020) eaba9636.

[107] Q. Gu, L. Shanahan, J.W. Hart, S. Belser, N. Shofer, M. Atature, H.S. Knowles, Simultaneous nanorheometry and nanothermometry using intracellular diamond quantum sensors, *ACS Nano* 17 (2023) 20034–20042.

[108] D.M. Toyli, C.F. de Las Casas, D.J. Christle, V.V. Dobrovitski, D.D. Awschalom, Fluorescence thermometry enhanced by the quantum coherence of single spins in diamond, *Proc. Natl. Acad. Sci.* 110 (2013) 8417–8421.

[109] J. Yun, K. Kim, S. Park, D. Kim, Temperature Selective Thermometry with Sub-Microsecond Time Resolution Using Dressed-Spin States in Diamond, *Adv. Quantum Technol.* 4 (2021) 2100084.

[110] L. Golubewa, Y. Padrez, S. Malykhin, T. Kulahava, E. Shamova, I. Timoshchenko, M. Franckevicius, A. Selskis, R. Karpicz, A. Obraztsov, All-Optical Thermometry with NV and SiV Color Centers in Biocompatible Diamond Microneedles, *Adv. Opt. Mater.* 10 (2022) 2200631.

[111] N. Wang, G.-Q. Liu, W.-H. Leong, H. Zeng, X. Feng, S.-H. Li, F. Dolde, H. Fedder, J. Wrachtrup, X.-D. Cui, Magnetic criticality enhanced hybrid nanodiamond thermometer under ambient conditions, *Phys. Rev. X* 8 (2018) 011042.

[112] C.-F. Liu, W.-H. Leong, K. Xia, X. Feng, A. Finkler, A. Denisenko, J. Wrachtrup, Q. Li, R.-B. Liu, Ultra-sensitive hybrid diamond nanothermometer, *Natl. Sci. Rev.* 8 (2020).

[113] P.-C. Tsai, C.P. Epperla, J.-S. Huang, O.Y. Chen, C.-C. Wu, H.-C. Chang, Measuring Nanoscale Thermostability of Cell Membranes with Single Gold-Diamond Nanohybrids, *Angew. Chem. Int. Ed.* 56 (2017) 3025–3030.

[114] S. Sotoma, C. Zhong, J.C.Y. Kah, H. Yamashita, T. Plakhotnik, Y. Harada, M. Suzuki, In situ measurements of intracellular thermal conductivity using heater-thermometer hybrid diamond nanosensors, *Sci. Adv.* 7 (2021) eabd7888.

[115] J. Choi, H. Zhou, R. Landig, H.-Y. Wu, X. Yu, S.E. Von Stetina, G. Kucska, S. E. Mango, D.J. Needleman, A.D. Samuel, Probing and manipulating embryogenesis via nanoscale thermometry and temperature control, *Proc. Natl. Acad. Sci.* 117 (2020) 14636–14641.

[116] E.N. Gerasimova, L.I. Fatkhutdinova, I.I. Vazhenin, E.I. Uvarov, E. Vysotina, L. Mikhailova, P.A. Lazareva, D. Kostyushev, M. Abakumov, A. Parodi, Hybrid plasmonic nanodiamonds for thermometry and local photothermal therapy of melanoma: a comparative study, *Nanophotonics* 13 (2024) 4111–4125.

[117] L. Ma, J. Zhang, Z. Hao, J. Jing, T. Zhang, Y. Lin, Z. Chu, A Diamond Heater-Thermometer Microsensor for Measuring Localized Thermal Conductivity: A Case Study in Gelatin Hydrogel, *Adv. Opt. Mater.* 2401232 (2024).

[118] S. Choi, V.N. Agafonov, V.A. Davydov, T. Plakhotnik, Ultrasensitive all-optical thermometry using nanodiamonds with a high concentration of silicon-vacancy centers and multiparametric data analysis, *ACS Photonics* 6 (2019) 1387–1392.

[119] J. Zhao, K. Babiuch, H. Lu, A. Dag, M. Gottschaldt, M.H. Stenzel, Fructose-coated nanoparticles: a promising drug nanocarrier for triple-negative breast cancer therapy, *Chem. Commun.* 50 (2014) 15928–15931.

[120] W. Jiang, B.Y.S. Kim, J.T. Rutka, W.C.W. Chan, Nanoparticle-mediated cellular response is size-dependent, *Nat. Nanotechnol.* 3 (2008) 145–150.

[121] B.D. Chithrani, W.C.W. Chan, Elucidating the Mechanism of Cellular Uptake and Removal of Protein-Coated Gold Nanoparticles of Different Sizes and Shapes, *Nano Lett.* 7 (2007) 1542–1550.

[122] B.D. Chithrani, A.A. Ghazani, W.C.W. Chan, Determining the Size and Shape Dependence of Gold Nanoparticle Uptake into Mammalian Cells, *Nano Lett.* 6 (2006) 662–668.

[123] J. Zhao, H. Lai, H. Lu, C. Barner-Kowollik, M.H. Stenzel, P. Xiao, Fructose-Coated Nanodiamonds: Promising Platforms for Treatment of Human Breast Cancer, *Biomacromolecules* 17 (2016) 2946–2955.

[124] W. Liu, M.N.A. Alam, Y. Liu, V.N. Agafonov, H. Qi, K. Koynov, V.A. Davydov, R. Uzbekov, U. Kaiser, T. Lasser, F. Jelezko, A. Ermakova, T. Weil, Silicon-Vacancy Nanodiamonds as High Performance Near-Infrared Emitters for Live-Cell Dual-Color Imaging and Thermometry, *Nano Lett.* 22 (2022) 2881–2888.

[125] X. Di, D. Wang, J. Zhou, L. Zhang, M.H. Stenzel, Q.P. Su, D. Jin, Quantitatively monitoring in situ mitochondrial thermal dynamics by upconversion nanoparticles, *Nano Lett.* 21 (2021) 1651–1658.

[126] Z. Ge, Q. Li, Y. Wang, Free Energy Calculation of Nanodiamond-Membrane Association—The Effect of Shape and Surface Functionalization, *J. Chem. Theory Comput.* 10 (2014) 2751–2758.

[127] Z. Chu, S. Zhang, B. Zhang, C. Zhang, C.-Y. Fang, I. Rehori, P. Cigler, H.-C. Chang, G. Lin, R. Liu, Q. Li, Unambiguous observation of shape effects on cellular fate of nanoparticles, *Sci. Rep.* 4 (2014) 4495.

[128] T. Schröder, M.E. Trusheim, M. Walsh, L. Li, J. Zheng, M. Schukraft, A. Sipahigil, R.E. Evans, D.D. Sukachev, C.T. Nguyen, J.L. Pacheco, R.M. Camacho, E. S. Bielejec, M.D. Lukin, D. Englund, Scalable focused ion beam creation of nearly lifetime-limited single quantum emitters in diamond nanostructures, *Nat. Commun.* 8 (2017) 15376.

[129] T. Zhang, L. Ma, L. Wang, F. Xu, Q. Wei, W. Wang, Y. Lin, Z. Chu, Scalable Fabrication of Clean Nanodiamonds via Salt-Assisted Air Oxidation: Implications for Sensing and Imaging, *ACS Appl. Nano Mater.* 4 (2021) 9223–9230.

[130] D. Terada, F.T.K. So, B. Hattendorf, T. Yanagi, E. Ōsawa, N. Mizuochi, M. Shirakawa, R. Igarashi, T.F. Segawa, A simple and soft chemical deaggregation method producing single-digit detonation nanodiamonds, *Nanoscale Adv.* 4 (2022) 2268–2277.

[131] J. Zhao, M. Lu, H. Lai, H. Lu, J. Lalevée, C. Barner-Kowollik, M.H. Stenzel, P. Xiao, Delivery of amonafide from fructose-coated nanodiamonds by oxime ligation for the treatment of human breast cancer, *Biomacromolecules* 19 (2018) 481–489.

[132] H.J. Shulevitz, A. Amirshaghaghi, M. Ouellet, C. Brustoloni, S. Yang, J.J. Ng, T.-Y. Huang, D. Jishkariani, C.B. Murray, A. Tsourkas, Nanodiamond emulsions for enhanced quantum sensing and click-chemistry conjugation, *ACS Appl. Nano Mater.* 7 (2024) 15334–15343.

[133] Y. Wu, F. Jelezko, M.B. Plenio, T. Weil, Diamond quantum devices in biology, *Angew. Chem. Int. Ed.* 55 (2016) 6586–6598.

[134] N. Kang, S. Son, S. Min, H. Hong, C. Kim, J. An, J.S. Kim, H. Kang, Stimuli-responsive ferropotosis for cancer therapy, *Chem. Soc. Rev.* 52 (2023) 3955–3972.

[135] Z. Wang, Z. Tian, Y. Dong, L. Li, L. Tian, Y. Li, B. Yang, Nanodiamond-conjugated transferrin as chemotherapeutic drug delivery, *Diam. Relat. Mater.* 58 (2015) 84–93.

[136] Y. Wu, A. Ermakova, W. Liu, G. Pramanik, T.M. Vu, A. Kurz, L. McGuinness, B. Naydenov, S. Hafner, R. Reuter, Programmable biopolymers for advancing biomedical applications of fluorescent nanodiamonds, *Adv. Funct. Mater.* 25 (2015) 6576–6585.

[137] X. Du, L. Li, S. Wei, S. Wang, Y. Li, A tumor-targeted, intracellular activatable and theranostic nanodiamond drug platform for strongly enhanced in vivo antitumor therapy, *J. Mater. Chem. B* 8 (2020) 1660–1671.

[138] S. Lee, M.S. Kim, K.D. Patel, H. Choi, R. Thangam, J. Yoon, T.M. Koo, H.J. Jung, S. Min, G. Bae, Magnetic Control and Real-Time Monitoring of Stem Cell Differentiation by the Ligand Nanoassembly, *Small* 17 (2021) 2102892.

[139] M.J. Ko, W. Yoo, S. Min, Y.S. Zhang, J. Joo, H. Kang, D.-H. Kim, Photonic control of image-guided ferropotosis cancer nanomedicine, *Coord. Chem. Rev.* 500 (2024) 215532.

[140] H. Li, M. Ma, J. Zhang, W. Hou, H. Chen, D. Zeng, Z. Wang, Ultrasound-enhanced delivery of doxorubicin-loaded nanodiamonds from pullulan-all-trans-retinal nanoparticles for effective cancer therapy, *ACS Appl. Mater. Interfaces* 11 (2019) 20341–20349.

[141] R. Selvam, A. Gandhi, S.-C. Hung, A.V. Karmenyan, E. Perevedentseva, W.-C. Yeh, S.-Y. Wu, H.-H. Chang, C.-L. Cheng, Multifunctional ferromagnetic nanodiamond for dual-mode fluorescence imaging and magnetic drug targeting, *Diam. Relat. Mater.* 139 (2023) 110398.

[142] H.M. Leung, L.S. Liu, Y. Cai, X. Li, Y. Huang, H.C. Chu, Y.R. Chin, P.K. Lo, Light-Activated Nanodiamond-Based Drug Delivery Systems for Spatiotemporal Release of Antisense Oligonucleotides, *Bioconjug. Chem.* 35 (2024) 623–632.